ELSEVIER

Polymer 43 (2002) 1503–1525

polymer

www.elsevier.com/locate/polymer

Application of statistical mechanics to the analysis of various physical properties of elastomeric networks — a review ☆

A. Kloczkowski

Laboratory of Experimental and Computational Biology, National Cancer Institute, National Institutes of Health, 12 South Drive, Bldg 12B, Rm B116, Bethesda, MD 20892-567, USA

Abstract

This paper examines the application of the statistical mechanics to the analysis of various physical properties of the elastomeric networks. The equilibrium properties of rubber-like networks are discussed, and also some dynamic properties, such as the relaxation spectrum of Gaussian networks. The paper covers a large spectrum of properties of polymer networks such as: fluctuations and chain dimensions in unimodal and bimodal network, effects of entanglements and constraints on the elastic properties of the network, segmental orientation, liquid-crystalline networks, small angle neutron scattering from networks, strain birefringence, elastic properties of filled networks, strain induced crystallization etc. The paper shows that the statistical mechanics can be successfully used to the analysis of almost all physical properties of rubber-like networks. © 2001 Published by Elsevier Science Ltd.

Keywords: Elastomeric networks; Physical properties; Statistical mechanics

1. Introduction

Elastomeric polymers are materials that are commonly used in everyday life. A better understanding of structure and properties of elastomers is therefore an important scientific and technological problem the can lead to the improvement of various properties of the known elastomeric materials, and to the development of completely new high performance polymers.

The subject of this paper is theoretical analysis of elastomeric networks based on statistical mechanics. The coverage is restricted mostly to equilibrium properties of networks, with the exception of theoretical analysis of the relaxation spectrum of Gaussian networks. The dynamical problem of the relaxation of Gaussian networks is directly related to the eigenvalue problem of Kirchhoff martices for the network, covered in detail in this work, so it was natural to include this problem in this paper.

The structure of this paper is the following: Section 2 has introductory character and is an overview of various classical theories of rubber elasticity. In the later part of this work the theory of phantom Gaussian networks is discussed in detail.

The phantom Gaussian network model is a fundamental concept in the theory of rubber-like elasticity and is used by advanced theories of real networks as a reference state upon which these more realistic models are built. The rigorous analytical results for this model are presented in Section 3. Section 4 shows the application of these results to the theoretical analysis of small angle neutron scattering from unimodal polymer networks

Section 5 contains the theoretical analysis of bimodal networks, i.e. networks composed of two types of chains: long and short ones. Recently it has been found that the bimodal distribution of polymer chains can be used to improve mechanical properties of high performance elastomeric material. The basic theoretical analysis of these networks is therefore important from the point of view of possible industrial applications of these materials.

Section 6 contains the study of dynamic properties of Gaussian networks, based on the eigenvalue analysis of Kirchhoff matrices. The new more realistic theory has been presented, which extends the classical theory of Graessley by taking into account the internal structure of network chains. This new theory gives much better insight into the dynamics of real networks and has been recently applied by various experimental groups to the analysis of data on the dynamics of elastomers.

Section 7 gives the theoretical analysis of the effect

☆ This paper was originally submitted to *Computational and Theoretical Polymer Science* and received on 29 October 2000; received in revised form on 9 July 2001; accepted on 9 July 2001. Following the incorporation of *Computational and Theoretical Polymer Science* into *Polymer*, this paper was consequently accepted for publication in *Polymer*.

E-mail address: kloczkoa@mail.nih.gov (A. Kloczkowski).

0032-3861/02/$ - see front matter © 2001 Published by Elsevier Science Ltd.
PII: S0032-3861(01)00588-2

of constraints along polymer chains on the elastic properties on rubber-like materials. The new 'diffused-constraint' theory of rubber elasticity, which is an extension of the classical constraint theory of Flory is presented. Flory assumed that constraints are localized and effect only fluctuations of network junctions. The new theory is more realistic since it takes into account the effect of constraints on the fluctuations of both network chains and network junctions.

Section 8 contains the theoretical analysis of segmental orientation, and polymer networks composed of semi-rigid chains. Such liquid-crystalline networks have very interesting properties because of the possibility of the isotropic–nematic phase transition induced by stretching the networks, or by deswelling it. Mechanically driven phase transitions are extremely interesting both from the fundamental point of view and because of various possibilities of practical application.

In Section 9 the strain-induced crystallization in elastomeric networks has been studied. The classical Flory theory of strain-induced crystallization has been extended by incorporating the effects of constrains on the elastic properties of network chains.

Section 10 has been devoted to the theoretical analysis of filled polymer networks. This is a very important problem, because fillers such as silica or carbon back are commonly used to improve mechanical properties of elastomers, and there is no molecular theory of filled elastomers. The new theory of reinforcement by filler particles has been developed, by studying the effect of the excluded volume of particles on the distribution of the end-to-end vector of polymer chains.

In Section 11 a discussion of perspectives and possible new developments in the statistical mechanics of rubber-like networks is presented.

This paper is based on my work done in the time period 1987–1994 at the Polymer Research Center at the Department of Chemistry of the University of Cincinnati, where I had great pleasure in working with Professor James E. Mark. Professor James E. Mark is the founder of the University of Cincinnati Polymer Research Center and is one of the most eminent scholars in the field of rubber-like elasticity. It was my great honor to collaborate with him, and make several theoretical contributions to the field of rubber-like elasticity. I would like also to acknowledge very fruitful collaboration with Professor Burak Erman who was frequently visiting University of Cincinnati. Professor Erman was a longtime collaborator of the late Nobel Prize Winner Paul J. Flory. Professor James E. Mark was also associated with Flory during his postdoctoral work in sixties. Many of the ideas and theories which were developed at the University of Cincinnati in collaboration with Professors J.E. Mark and B. Erman, such as theory of chain dimensions, or the diffused constraints theory of rubber elasticity were inspired by fundamental pioneering works of Flory.

2. Overview of classical theories of rubber elasticity

2.1. Kuhn–Treloar theory

The first theoretical molecular approach to the theory of rubber elasticity was done by Kuhn in late thirties [1–3]. Other important early contributions to the early rubber elasticity theory were seminal papers by Meyar, von Susich and Valko [113] and by Guth and Mark [114]. A very good review of history of early rubber elasticity was given by Flory [115]. The theory Kuhn, Guth, Mark approach was further developed by Treloar [4–5].

This element approach is based on the assumptions that the rubber network consists on ν freely-jointed Gaussian chains. It is assumed that crosslinking of chains in the undeformed network does not change mean square end-to-end distance of chains in respect to the uncrosslinked polymer melt. This assumption is supported by data obtained from neutron scattering experiments [6–8].

Another assumption is that the volume of the rubber network does not change during the stretching, and that positions of junctions (points of crosslinking) deform affinely upon deformation. It is also assumed that the total free energy of the network is the sum of free energies of all ν chains.

The elastic free energy of the deformed network is

$$\Delta A_{\mathrm{el}} = \frac{3kT}{2\langle r^2\rangle_0}\sum_{\nu}(r^2 - \langle r^2\rangle_0) = \frac{3\nu kT}{2}\left(\frac{\langle r^2\rangle}{\langle r^2\rangle_0} - 1\right) \quad (1)$$

writing $\langle r^2\rangle$ in terms of the Cartesian components of the deformation tensor $\boldsymbol{\lambda}$ we obtain:

$$\langle \mathbf{r}^2\rangle = \langle x^2\rangle + \langle y^2\rangle + \langle z^2\rangle = \frac{1}{3}\langle r^2\rangle_0\left(\lambda_x^2 + \lambda_y^2 + \lambda_z^2\right) \quad (2)$$

which leads to

$$\Delta A_{\mathrm{el}} = \frac{1}{2}\nu kT\left(\lambda_x^2 + \lambda_y^2 + \lambda_z^2 - 3\right) \quad (3)$$

The elastic force f is then

$$f = \left(\frac{\partial \Delta A_{\mathrm{el}}}{\partial L}\right)_{T,V} = \frac{1}{L_0}\left(\frac{\partial \Delta A_{\mathrm{el}}}{\partial \lambda}\right)_{T,V} = \frac{\nu kT}{L_0}(\lambda - \lambda^{-2}) \quad (4)$$

where $\lambda = \lambda_x$ is the x-component of the deformation tensor $\boldsymbol{\lambda}$ (assuming that the rubber is stretched in the x direction), and L_0 is the length of the undeformed rubber sample in the direction of stretch.

The Khun–Treloar theory is very simple but gives pretty good description of experimental data [6,9].

2.2. James and Guth theory of phantom networks

The theory of phantom networks was developed in the forties by James and Guth [10–17]. They assumed that the network is composed of crosslinked Gaussian chains. They assumed that there are two types of network junctions. Junctions which are at the surface of the rubber are fixed and

deform affinely with the macrospcopic strain, while the junctions inside the network are free to fluctuate around their mean positions. They assumed also that the behavior of the network is determined only by the connectivity of network chains. James and Guth neglected the effect of the excluded volume of polymer chains. The chains in their model are phantom-like, i.e. they may pass freely through each other.

The configurational partition function Z_N of the network is the product of configurational particle functions of network Gaussian chains [18]:

$$Z_N = C\prod_{i<j}\exp\left[\frac{1}{2}\sum_i\sum_j \gamma_{ij}(\mathbf{R}_i - \mathbf{R}_j)^2\right] \tag{5}$$

where C is a normalization constant and the matrix elements γ_{ij} ($\gamma = -\gamma'$) are defined as:

$$\gamma_{ij} = \left\{\begin{array}{c} \dfrac{3}{2\langle r_{ij}^2\rangle_0} \text{ if } i \text{ and } j \text{ are connected by a chain} \\ 0 \text{ if } i \text{ and } j \text{are not connected} \end{array}\right\} \tag{6}$$

This means that all statistical properties of the network depend on the connectivity matrix $\mathbf{\Gamma}$ defined by the above Eq. (6) [19]. One can easily calculate fluctuations of junctions in the phantom network model, and correlations between these fluctuations for the ideal infinite network with the topology of the tree (with functionality ϕ of network junctions). These quantities are related to the matrix elements of the inverse matrix $\mathbf{\Gamma}^{-1}$. The mean square fluctuations of the end-to-end vector $\langle(\Delta r)^2\rangle$ of polymer chains depend on the functionality ϕ of the network and is given by the formula [20]:

$$\langle(\Delta r)^2\rangle = \frac{2}{\phi}\langle r^2\rangle_0 \tag{7}$$

These fluctuations are assumed to be independent of the macroscopic strain. The mean square end-to-end vector of the chain $\langle(r_{ij})^2\rangle$ between junctions i and j can be written as:

$$\langle(r_{ij})^2\rangle = \langle(\overline{r_{ij}})^2\rangle + \langle(\Delta r_{ij})^2\rangle \tag{8}$$

where $\langle(\overline{r_{ij}})^2\rangle$ is the time averaged mean square end-to-end vector, and $\langle(\Delta r_{ij})^2\rangle$ represents instantaneous fluctuations in the chain vector $\mathbf{r}_{ij}$ from its average value $\overline{\mathbf{r}_{ij}}$. It is also assumed that average vectors transform affinely with the macroscopic deformation of the rubber, i.e.

$$\begin{aligned}\langle(\overline{r_{ij}})^2\rangle &= \lambda_x^2\langle(\overline{x_{ij}})^2\rangle_0 + \lambda_y^2\langle(\overline{y_{ij}})^2\rangle_0 + \lambda_z^2\langle(\overline{z_{ij}})^2\rangle_0 \\ &= \frac{1}{3}\langle(\overline{r_{ij}})^2\rangle_0\left(\lambda_x^2 + \lambda_y^2 + \lambda_z^2\right)\end{aligned} \tag{9}$$

Because of this the elastic free energy of the phantom network in the formulation by Flory [18] is

$$\Delta A_{\mathrm{el,ph}} = \frac{1}{2}\xi kT\left(\lambda_x^2 + \lambda_y^2 + \lambda_z^2 - 3\right) \tag{10}$$

where ξ is so-called cycle rank [21,22] of the perfect tree-like network defined as:

$$\xi = \left(1 - \frac{2}{\phi}\right)\nu \tag{11}$$

where ϕ is the functionality of junctions in the network (the number of chains connected at each junction) and ν is the number of chains. Originally, according to the mathematical graph theory, for any (even imperfect) network the cycle rank is given as the number of scissions necessary to reduce the graph to a spanning tree. By comparing Eq. (11) with Eq. (3) for the Kuhn–Treloar theory, we see that the main difference in the elastic free energy is due to the $2\nu/\phi$ term which is related to the strain independent fluctuations of the network.

The more detailed analysis of the phantom network theory will be given in the following sections.

2.3. Affine model of rubber elasticity of Wall and Flory

The affine theory developed by Wall and by Flory [23–29] assumes that junctions of the network transform affinely with macroscopic strain. The expression of the elastic free energy is similar to Eq. (3) of the theory of Kuhn. In the case of swelling of the network there is an extra logarithmic term associated with the volume change of the rubber

$$\Delta A_{\mathrm{el}} = \frac{1}{2}\nu kT\left(\lambda_x^2 + \lambda_y^2 + \lambda_z^2 - 3\right) - \frac{2\nu}{\phi}kT\ln\left(\frac{V}{V_0}\right) \tag{12}$$

where V is the volume of the network, and V_0 is the volume of the network in the reference state in which the network was formed. Here ν is the number of chains and ϕ is the network functionality. The affine model of the rubber elasticity is very important, because it is a fundamental limiting case in the constrained-junction theory of rubber elasticity of Flory.

2.4. Constrained-junction theory or rubber elasticity of Flory

In 1976 Flory published a theory of rubber elasticity, which takes into consideration chain entanglements and constraints occurring in real (non-phantom) polymer networks [30]. The effects of constraints were also studied earlier by Ranca and Allegra [31] and by Kaestner [116–118]. The history of theoretical approach to this problem is given by Burchard [119] and by Heinrich, Straube and Helmis [120].

The main idea of Flory theory is that constraints effect fluctuations of network junctions, compared to phantom-like state of reference. This effect of constraining fluctuations of junctions is measured by a parameter κ in the theory defined as:

$$\kappa = \frac{\langle(\Delta R)^2\rangle_{\mathrm{ph}}}{\langle(\Delta s)^2\rangle} \tag{13}$$

where $\langle(\Delta R)^2\rangle_{\mathrm{ph}}$ are mean square fluctuations of junctions in

the phantom network, and $\langle(\Delta s)^2\rangle$ is a mean square fluctuation in the Gaussian distribution of centers of entanglements in the undeformed state. As a result the constrained-junction theory of Flory is intermediate between the phantom network model and the affine network model. The elastic free energy in the theory is given by the following expression:

$$\Delta A_{\mathrm{el}} = \frac{1}{2}\xi kT \sum_{t=x,y,z} \left\{ \left(\lambda_t^2 - 1\right) + \frac{\mu}{\xi}[B_t + D_t - \ln(B_t + 1) - \ln(D_t + 1)] \right\} \quad (14)$$

where μ is the number of junctions, ξ is the cycle rank (see Eq. (11)) and B_t and D_t are defined as:

$$B_t = \frac{\kappa^2\left(\lambda_t^2 - 1\right)}{\left(\lambda_t^2 + \kappa\right)^2} \quad t = x, y, z \quad (15)$$

$$D_t = \lambda_t^2 \frac{B_t}{\kappa} \quad t = x, y, z \quad (16)$$

It is easy to show that in the limit $\kappa = 0$ the elastic free energy in the constrained-junction model becomes identical as in the phantom network model (Eq. (10)), while in the limit $\kappa \rightarrow \infty$ it is similar as in the theory of affine networks (Eq. (12)).

The parameter κ of the constrained junction model can be interpreted in terms of the molecular constitution of the network as [32]

$$\kappa = I \frac{2N_{\mathrm{A}}d}{\phi}\left(\frac{\langle r^2\rangle_0}{M}\right)^{3/2} M_{\mathrm{c}}^{1/2} \quad (17)$$

where I is proportionality constant, ϕ is the functionality of the network, N_{A} is Avogadro number, d is the network density, M_{c} is the molecular weight of a chain with end-to-end mean square length $\langle r^2\rangle_0$. The constrained chain theory was refined later by Erman and Flory [33,34].

2.5. Edwards replica and tube theories

A different approach to the rubber elasticity was developed by Deam and Edwards in 1976 [35]. The Edwards approach is based on his earlier works on replica theory developed for solid-state physics in application to amorphous systems. The replica method has been introduced by Edwards to perform statistical mechanics averaging for amorphous systems subject to both internal and external constraints. Because the theory leads to complicated mathematics, the details are skipped here. The main advantage of this approach is that crosslinks could be considered in detail, and various approximations can reduce this theory to other classical theories. The affine and phantom networks become also limiting cases of the Edwards and Deam theory of rubber elasticity.

The replica method was used later by Ball, Doi and Edwards to develop the slip-link model of rubber elasticity [36]. They calculated the effects of entanglements along the chain contour on the elastic free energy. The slip-link may slide along the chain contour and is equivalent to an additional crosslink in the network. The final expression for the elastic free energy in this model is

$$\Delta A_{\mathrm{el}} = \frac{1}{2}N_{\mathrm{c}}kT\left\{ \sum_{t=x,y,z} \lambda_t^2 + \frac{N_{\mathrm{s}}}{N_{\mathrm{c}}} \times \sum_{t=x,y,z}\left[\frac{(1+\eta)\lambda_t^2}{1+\eta\lambda_t^2} + \ln\left(1+\eta\lambda_t^2\right)\right]\right\} \quad (18)$$

where N_{c} and N_{s} are the number of chemical crosslinks and sliplinks, respectively, and $\eta = 0.234$. The slip-link model has been later modified by Edwards and Vilgis [150].

Another model developed by Edwards is the tube model [136] based on the idea of harmonic-like tube constrains in elastomeric networks. This idea have been applied by de Gennes [137,138] within the framework of reptation theory, to the dynamics of uncrosslinked polymer melt. According to the tube theory polymer is trapped inside a tube of diameter a and length L, formed by constraints from neighboring crosslinks and chains. The elastic free energy in the tube model is larger than the free energy in the Kuhn model, because of the additional contribution of entanglements to the elastic modulus. A good review of tube model theories is given by Edwards and Vilgis [39].

The excluded volume interactions for polymer chains have been studied by Muthukumar [133,134] and Freed [135].

2.6. Other theories of rubber elasticity

In 1963 Brodowsky and Prager [106] developed a Debye–Hucke-like theory of a polymer network by treating it as a mixture of crosslinks with infinite functionality with bifunctional monomer. A similar approach has been recently used by Paul, Schulz and Frish [107] who derived the equation of state of a Gaussian phantom network by assuming that the network is a gas-like mixture of crosslinks with defined functionality and Guassian chains.

The main idea of tube model proposed originally by Edwards [136] and discussed earlier has been used by several other authors.

Marruchi, [139] Gaylord and Douglas, [140,141] Heinrich Straube and Helmis [120] and most recently Rubinstein and Panyukov [142] developed tube-type theories very successfully in the theoretical interpretation of the experimental data. In all these theories the free energy is a sum of a Gaussian term due to the chain connectivity and additional term due to entanglements. The difference between these theories arises mostly by using different assumptions about the dependence of the tube diameter on the macroscopic deformation.

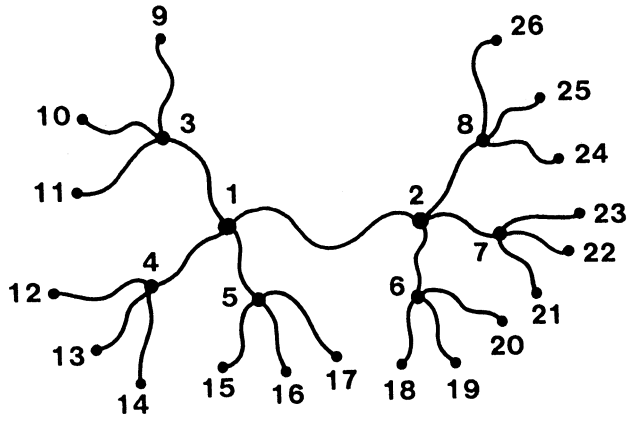

Fig. 1. First three tiers of a unimodal, symmetrically grown treelike network with functionality $\phi = 4$.

Eichinger have applied many concepts from the mathematical graph theory especially the concept of the Kirchhoff matrices to the theory of rubber elasticity [143–145].

Gressley [146,147,149] developed a model of restricted junction fluctuations based on a concept of trapped entanglements proposed by Langley [148]. It is assumed that during the crosslinking process some entanglements are 'trapped' and act as physical junctions.

Polymer networks have been studied extensively by computer simulations, although simulations of crosslinked polymer networks are much more difficult than simulations of uncrosslinked polymer chains. A very good review of this subject is given by Kremer and Grest [124]. The simulations of dense polymer networks were performed by using both Monte Carlo [125] and molecular dynamics [126] methods. The elastic properties of networks and the effect of topological constrains have been studied extensively by Kremer and Everaers in a series of papers [127–132].

3. Chain dimensions and fluctuations in random elastomeric networks

Chain dimensions and fluctuations in random elastomeric networks were studied by Kloczkowski, Mark and Ernam [37,38]. The behavior of phantom Gaussian networks in the underformed state was studied in detail. The partition function of the phantom network is

$$Z_{N_\tau} = C \exp[-\{\Delta\mathbf{R}_\tau\}^T \mathbf{\Gamma}_\tau \{\Delta\mathbf{R}_\tau\}] \tag{19}$$

where $\{\Delta\mathbf{R}_\tau\}$ is the vector of fluctuations of the set $\{\tau\}$ of the free junctions, and $\mathbf{\Gamma}_\tau$ is the connectivity matrix with elements γ_{ij} defined as

$$\gamma_{ij} = \begin{cases} \dfrac{-3}{2\langle \mathbf{r}_{ij}^2 \rangle_0} & \text{if } i \text{ and } j \text{ are connected by a chain} \\ 0 & \text{if } i \text{ and } j \text{ are not connected} \end{cases} \tag{20}$$

and the diagonal elements are defined such that the summation of all matrix elements in a given row (or column) is zero

$$\gamma_{ii} = -\sum_j \gamma_{ij} \tag{21}$$

It can be shown that the fluctuation of a junction i, $\langle(\Delta R_i)^2\rangle$ is related to the element Γ_{ij}^{-1} of the inverse of the connectivity matrix $\mathbf{\Gamma}$, and more generally the correlations $\langle(\Delta\mathbf{R}_i \cdot \Delta\mathbf{R}_j)\rangle$ are related to Γ_{ij}^{-1}

$$\langle(\Delta\mathbf{R}_i \cdot \Delta\mathbf{R}_j)\rangle = \frac{3}{2}\Gamma_{ij}^{-1} \tag{22}$$

The elements of the inverse matrix were calculated analytically for the network with the topology of the infinite tree, composed of chains of equal length (unimodal network), with equal mean square end-to-end distances $\langle r^2\rangle_0$ in the undeformed state. It was assumed that the network has functionality ϕ, i.e. that each free junction connects exactly ϕ chains. Fig. 1 shows an example of such a tree-like network with functionality $\phi = 4$. It is possible to derive the recurrence relations between fluctuations of junctions in the neighboring tiers of the tree. The simplest case is when junctions i and j are directly connected by a singly chain. For the infinite tree (infinite number of tiers) of unimodal chains the solution of the problem converges to the following simple formula

$$\begin{bmatrix} \langle(\Delta R_i)^2\rangle & \langle(\Delta\mathbf{R}_i \cdot \Delta\mathbf{R}_j)\rangle \\ \langle(\Delta\mathbf{R}_i \cdot \Delta\mathbf{R}_j)\rangle & \langle(\Delta R_j)^2\rangle \end{bmatrix} = \langle r^2\rangle_0 \begin{bmatrix} \dfrac{\phi-1}{\phi(\phi-2)} & \dfrac{1}{\phi(\phi-2)} \\ \dfrac{1}{\phi(\phi-2)} & \dfrac{\phi-1}{\phi(\phi-2)} \end{bmatrix} \tag{23}$$

where ϕ is the functionality of the network. Because of this fluctuations $\langle(\Delta r_{ij})^2\rangle$ of the distance r_{ij} between any two junctions i and j in the network connected by a single chain are

$$\langle(\Delta r_{ij})^2\rangle = \frac{2}{\phi}\langle r_{ij}^2\rangle_0 \tag{24}$$

In the case of two junctions m and n separated by d other junctions along the path joining m and n, the solution of the problem is

$$\begin{bmatrix} \langle(\Delta R_m)^2\rangle & \langle(\Delta\mathbf{R}_m \cdot \Delta\mathbf{R}_n)\rangle \\ \langle(\Delta\mathbf{R}_m \cdot \Delta\mathbf{R}_n)\rangle & \langle(\Delta R_n)^2\rangle \end{bmatrix} = \langle r^2\rangle_0 \begin{bmatrix} \dfrac{\phi-1}{\phi(\phi-2)} & \dfrac{1}{\phi(\phi-2)(\phi-1)^d} \\ \dfrac{1}{\phi(\phi-2)(\phi-1)^d} & \dfrac{\phi-1}{\phi(\phi-2)} \end{bmatrix} \tag{25}$$

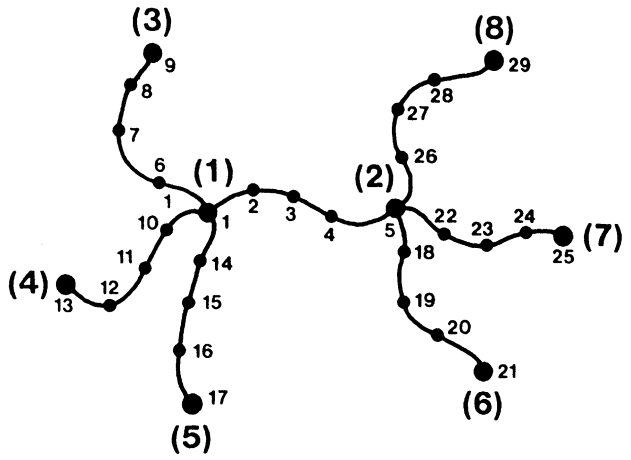

Fig. 2. Tetrafunctional network with additional bifunctional junctions which separate each chain into $n = 4$ subchains of equal length.

and the fluctuations $\langle(\Delta\mathbf{r}_{mn})^2\rangle$ of the distance r_{mn} are equal

$$\langle(\Delta\mathbf{r}_{mn})^2\rangle = \frac{2}{\phi(\phi-2)(d+1)}\,\frac{(\phi-1)^{d+1}-1}{(\phi-1)^d}\langle r_{mn}^2\rangle_0 \quad (26)$$

The problem can be also solved for the general case of fluctuations of points along the chains in the network and correlations of fluctuations among such points. To deal with this case we may assume that each chain between two ϕ functional junction is composed of n Gaussian segments connected by bifunctional junctions to form a chain as shown in Fig. 2. Because of this the diagonal elements γ_{ij} of the connectivity matrix are ϕ if the index i corresponds to the ϕ functional junction and 2 for the bifunctional junction. The off-diagonal elements γ_{ij} are -1 if i and j are directly connected by a chain segment, and zero otherwise.

Similarly as before the recursion relations between the elements of the inverse matrix $\mathbf{\Gamma}^{-1}$ can be derived. For the infinite number of tiers in the tree-like network the solution of the problem has the following form

$$\begin{bmatrix} \langle(\Delta R_i)^2\rangle & \langle(\Delta\mathbf{R}_i\cdot\Delta\mathbf{R}_j)\rangle \\ \langle(\Delta\mathbf{R}_i\cdot\Delta\mathbf{R}_j)\rangle & \langle(\Delta R_j)^2\rangle \end{bmatrix}$$
$$= \langle r^2\rangle_0 \begin{bmatrix} \dfrac{\phi-1}{\phi(\phi-2)} + \dfrac{\zeta(1-\zeta)(\phi-2)}{\phi} & \dfrac{1}{\phi(\phi-2)(\phi-1)^d} + \dfrac{[1+\zeta(\phi-2)][(\phi-1)-\theta(\phi-2)]}{\phi} \\ \dfrac{1}{\phi(\phi-2)(\phi-1)^d} + \dfrac{[1+\zeta(\phi-2)][(\phi-1)-\theta(\phi-2)]}{\phi} & \dfrac{\phi-1}{\phi(\phi-2)} + \dfrac{\theta(1-\theta)(\phi-2)}{\phi} \end{bmatrix} \quad (27)$$

Here $\zeta = i - 1/n$ and $\theta = j - 1/n$ are fractional distances of sites i and j from nearest ϕ-functional junctions on their left side (as shown in Fig. 3) with $0 < \zeta,\ \theta < 1$, and d is the number of ϕ-functional junctions between sites i and j. The above formula is also valid when i and j belong to the same chain (i.e $d = 0$) and $\zeta < \theta$.

Fluctuations $\langle(\Delta\mathbf{r}_{ij})^2\rangle$ of the distance r_{ij} are equal

$$\langle(\Delta r_{ij})^2\rangle = \left\{\frac{2(\phi-1)}{\phi(\phi-2)}\left[1 - \frac{1}{(\phi-1)^d}\right] + \frac{\phi-2}{\phi}\left[\zeta(1-\zeta) + \theta(1-\theta) - \frac{\zeta+\theta-2\zeta\theta}{(\phi-1)^d}\right] + \frac{\eta-d}{(\phi-1)^d}\right\}\langle r^2\rangle_0 \quad (28)$$

where $\eta = d + \theta - \zeta$ if point i is on the left side of point j (or $\eta = d + \zeta - \theta$ if point i is on the right side of point j). In a special case when points i and j are on the same chain (i.e. $d = 0$) then

$$\langle(\Delta r_{ij})^2\rangle = \left\{\eta - \frac{(\phi-2)}{\phi}\,\eta^2\right\}\langle r^2\rangle_0 \quad (29)$$

The above results are important for studies of elastic properties of phantom networks. It is assumed that instantaneous fluctuations of all distances in the network are independent of the macroscopic deformation, and only mean distances transform affinely with the deformation, i.e.

$$\overline{\mathbf{r}_{ij}} = \boldsymbol{\lambda}\overline{\mathbf{r}_{ij,0}} \quad (30)$$

Because of this the x-component of the mean-square end-to-end vector changes with deformation as

$$\langle\bar{x}^2\rangle = \lambda_x^2\left(1 - \frac{2}{\phi}\right)\langle x^2\rangle_0 \quad (31)$$

Similarly for two points i and j on a chain we have

$$\langle\bar{x}_{ij}^2\rangle = \lambda_x^2\left(1 - \frac{2}{\phi}\right)\langle\bar{x}_{ij}^2\rangle_0 = \frac{\eta}{3}\lambda_x^2\left(1 - \frac{2}{\phi}\right)\langle r^2\rangle_0 \quad (32)$$

Because most models of real networks use phantom network as a reference state for the construction of the real network models, these results are also important for real models of rubber elasticity. The most straightforward application is the analysis of the small angle neutron scattering from labeled paths in the rubber network.

Fig. 3. Two points l and j of the network separated by $d = 3$ tetrafunctional junctions. The positions of points l and j are measured with respect to the nearest multifunctional junction from the left as fractions ζ, θ of the contour length of the chain between multifunctional junctions.

4. Small angle neutron scattering from random elastomeric networks

The small angle neutron scattering methods enable experimental verification of theories of rubber elasticity. The change of the shape of polymer chains under external deformation can be experimentally measured [7,8,40, 152,153]. Small number of polymer chains in the network is labeled by deuteration, and these chains are monitored during SANS experiments. The experiments measure the form factor $S(q)$ defined as:

$$S(\mathbf{q}) = N^{-2} \sum_{i,j=1}^{N} \int \mathrm{e}^{\mathrm{i}\mathbf{q}\cdot\mathbf{r}_{ij}} \Omega(\mathbf{r}_{ij}) \mathrm{d}\mathbf{r}_{ij} \tag{33}$$

where $\mathbf{q}$ is the scattering vector, $\Omega(\mathbf{r}_{ij})$ is the distribution function of scattering centers and the averaging is taken over all N labeled scattering centers. For Gaussian $\Omega(\mathbf{r}_{ij})$ the form factor is

$$S(\mathbf{q}) = N^{-2} \sum_{i,j=1}^{N} \exp\left[-\frac{q_x^2}{2}\langle x_{ij}^2\rangle - \frac{q_y^2}{2}\langle y_{ij}^2\rangle - \frac{q_z^2}{2}\langle z_{ij}^2\rangle \right] \tag{34}$$

The problem of SANS from labeled chain in the phantom network was studied first by Pearson in 1977 [20]. The same problem was later studied by Ullman [41,42]. Warner and Edwards [121] calculated the scattering form factor $S(\mathbf{q})$ of randomly crosslinked networks by using replica method. Pearson studied the scattering from a single labeled chain attached between multifunctional junctions. The fluctuations of the mean square distance between center i and j along the chain are given by Eq. (29) and the x-component of mean square distance between sites i and j changes upon deformation as

$$\langle x_{ij}^2\rangle = \left\{ \lambda_x^2 + \left(1 - \lambda_x^2\right) \frac{\langle \Delta x_{ij}^2\rangle_0}{\langle x_{ij}^2\rangle_0} \right\} \langle x_{ij}^2\rangle_0 \tag{35}$$

and so therefore

$$\langle x_{ij}^2\rangle = \frac{1}{3}\left\{ \eta\lambda_x^2 + \left(1 - \lambda_x^2\right)\left[\eta - \frac{(\phi - 2)}{\phi}\eta^2 \right] \right\} \langle r^2\rangle_0 \tag{36}$$

Eq. (36) (and similar equations for y and z components) can be substituted to Eq. (34), and summation over N can be replaced by integration leading to the following result obtained by Pearson [20]

$$S(\mathbf{q}) = 2\int_0^1 \mathrm{d}\eta\, (1 - \eta) \exp\left\{ -\upsilon\eta\left\{ 1 - \eta(1 - \boldsymbol{\lambda}^{*2}) \frac{\phi - 2}{\phi} \right\} \right\} \tag{37}$$

where $\upsilon = q^2\langle r^2\rangle_0/6$ and the vector $\boldsymbol{\lambda}^*$ is

$$\boldsymbol{\lambda}^* = \boldsymbol{\lambda}\mathbf{q}/q \tag{38}$$

i.e. $\boldsymbol{\lambda}^{*2} = (q_x^2\lambda_x^2 + q_y^2\lambda_y^2 + q_z^2\lambda_z^2)/q^2$. For scattering parallel to the direction of extension $\lambda^* = \lambda_\parallel$ and for scattering perpendicular to the direction of extension $\lambda^* = \lambda_\perp = 1/\sqrt{\lambda_\parallel}$. Pearson result is applicable only to a single chain with no crosslinks along the labeled path.

These results were generalized by considering a labeled path with several multifunctional junctions [43–45]. By using Eq. (28) for fluctuations of points i and j separated by d ϕ-functional junctions the following equation for the form factor $S(\mathbf{q})$ can be derived

$$\begin{aligned} S(\mathbf{q}) = \frac{1}{n^2} \sum_{n_i=1}^{n} \sum_{n_j=1}^{n} \int_0^1 \mathrm{d}\theta \int_0^1 \mathrm{d}\zeta \exp\Bigg\{ -\upsilon\Bigg[\lambda^{*2}|n_j + \theta - n_i \\ + \zeta| + (1 - \lambda^{*2})\Bigg[\frac{2(\phi - 1)}{\phi(\phi - 2)}\Bigg[1 - \frac{1}{(\phi - 1)^{|n_j - n_i|}} \Bigg] \\ + \frac{\phi - 2}{\phi}\Bigg[\zeta(1 - \zeta) + \theta(1 - \theta) - \frac{\zeta + \theta - 2\zeta\theta}{(\phi - 1)^{|n_j - n_i|}} \Bigg] \\ + \frac{\eta - |n_j - n_i|}{(\phi - 1)^{|n_j - n_i|}} \Bigg]\Bigg]\Bigg\} \end{aligned} \tag{39}$$

In the case when there are no crosslinks along the path ($d = 0$) this formula reduces to Eq. (37).

The scattering form factor given by Eq. (39) may be easily evaluated numerically. The results can be shown as Kratky plots of $q^2S(\mathbf{q})$ vs. the scattering vector for varying length of the labeled path both in the undeformed and deformed state. In the undeformed state $q^2S(\mathbf{q})$ decreases with increase in the length of the path. This is due to the fact that correlations between points on different chains decrease rapidly as the number of crosslinks separating them increases. The main contribution to the scattering form factor is by points belonging to the same chain.

Since $S(\mathbf{q})$ is given by the double sum $(1/n^2)\sum_{n_i=1}^{n}\sum_{n_j=1}^{n}$ and there are only n terms in the sum when $n_i = n_j$, $S(\mathbf{q})$ behaves approximately as n^{-1} for large number n of chains in the path. The Kratky plots for undeformed, unswollen networks show no maxima with respect to the scattering vector $\mathbf{q}$. Kratky plots for deformed, unswollen networks for scattering wave vector parallel to the direction of stretch also show no maxima, as shown in Fig. 4. For scattering in the direction perpendicular to the direction of stretch and for sufficiently long paths, a maximum is observed in the Kratky plots (see Fig. 5). This shows satisfactory agreement with experimental data, because experimental Kratky plots

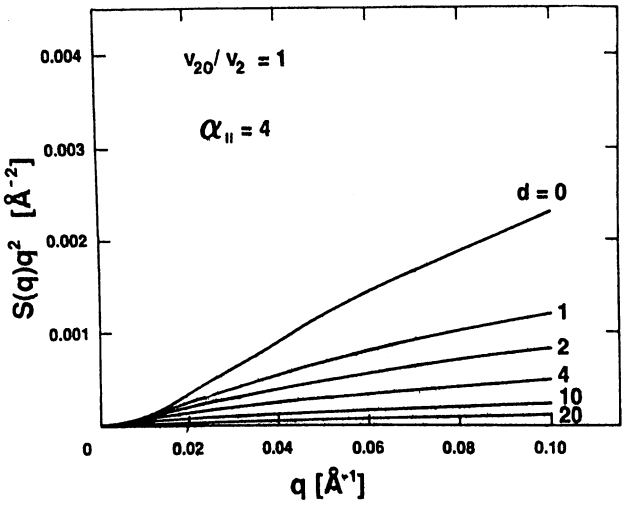

Fig. 4. Kratky plot for the unswollen deformed network ($\lambda_{\|} = 4$) for the scattering parallel to the principal axis of deformation for varying number d of cross links along the path.

show maxima for scattering from labeled paths in the direction perpendicular to the direction of stretch [46–48]. Such maximum does not exist for scattering from a single chain and this shows that this experimental maximum can be explained even by a simple phantom network model.

The problem of correlations among chains in a cross-linked path was studied in Ref. [44]. All authors studying the problem of SANS from labeled paths earlier used the assumption that different chain vectors along the path are uncorrelated both in the undeformed and in the deformed states. Ullman improved the theory by removing the assumption that different chain vectors of the path are uncorrelated in the deformed state [42]. However, in the undeformed state, he used the assumption that the different chain vectors are uncorrelated i.e. the path is freely

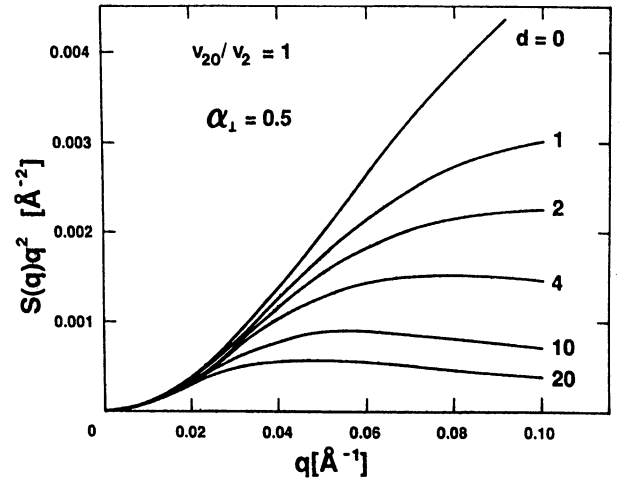

Fig. 5. Kratky plot for the unswollen deformed network ($\lambda_{\|} = 4$, i.e. $\lambda_{\perp} = 0.5$) for the scattering perpendicular to the principal axis of deformation for varying number d of crosslinks along the path.

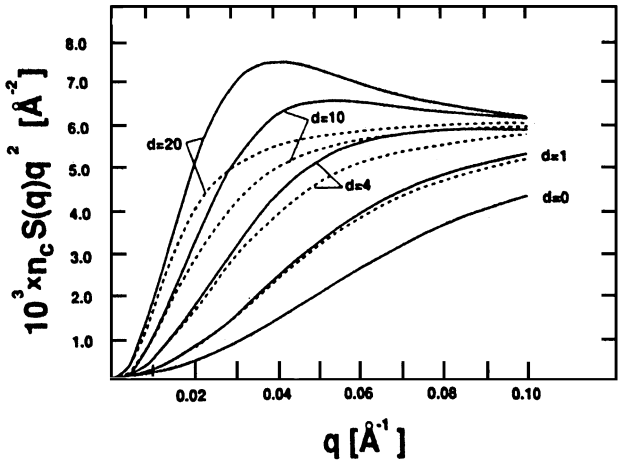

Fig. 6. The comparison of form factors obtained by using Eq. (41) (dashed lines) and Eq. (42) (solid lines) for labeled paths with varying number d of crosslinks along the path for the unswollen, undeformed ($\lambda = 1$) network.

jointed, so

$$\langle r_{ij}^2 \rangle_0 = \eta \langle r^2 \rangle_0 \tag{40}$$

where $\mathbf{r}_{ij}$ is the vector between points i and j on the path, $\mathbf{r}$ is the end-to-end vector for a chain between two consecutive cross-links along the path and η is the ratio of the contour length between i and j to that of a chain between two consecutive cross-links. In Eq. (40) angular brackets denote ensemble averages and the subscript zero identifies the undeformed state. For two instantaneous vectors $\mathbf{r}_{m,m+1}$ and $\mathbf{r}_{n,n+1}$ joining junctions m with $m + 1$ and n with $n + 1$ along a path, this assumption implies

$$\langle \mathbf{r}_{m,m+1} \cdot \mathbf{r}_{n,n+1} \rangle_0 = 0 \quad m \neq n \tag{41}$$

We replaced this assumption by

$$\langle \bar{\mathbf{r}}_{m,m+1} \cdot \bar{\mathbf{r}}_{n,n+1} \rangle_0 = 0 \quad m \neq n \tag{42}$$

where the overbar denotes time averaging. We think that Eq. (42) is more plausible for cross-linked paths in a phantom network. Eq. (42) postulates that in the undeformed state the distribution of the mean end-to-end vectors in the ensemble is isotropic. From the statistical–mechanical point of view the cross-linked system differs significantly from the uncross-linked one. Eq. (41) has been originally derived for free chains where both ensemble and time averages are the same. For the crosslinked system we must distinguish between time and ensemble averaging and the symmetry of the ensemble requires that Eq. (42) rather than Eq. (41) is satisfied. The scattering form factors $S(\mathbf{q})$ were calculated using both assumptions given by Eqs. (41) and (42). Fig. 6 compares the Kratky plots obtained by using these two different assumptions. For small number of crosslinks along the labeled path there is almost no difference for Kratky plots between these two assumptions. For larger number of crosslinks along the path Eq. (42) gives more pronounced maxima for scattering in the direction

perpendicular to the direction of stretch. The most interesting result is that the maximum on Kratky plot can be obtained for labeled path with many crosslinks even in the undeformed state. Most of experimental data show no maxima on Kratky plots for scattering from labeled paths in undeformed, unswollen networks, although in some cases a very small maximum may be observed. Our calculations have been performed for the phantom model of the polymer network. Real networks are not phantom. Entanglements and steric effects in real networks are very important and contribute even more significantly to the scattering properties of networks.

5. Bimodal networks

Most of the elastomeric networks studied theoretically are unimodal, which means that all chains have the same length. The unimodality of the network simplifies greatly analysis of the model. The unimodal network is also a good approximation for most of real networks where chains have no exactly the same length, but there is a distribution of chain lengths centered about a single mean value. The recent advance in network synthesis enables formation of bimodal networks composed of two types of chain: long and short ones. Such bimodal networks show interesting elastic properties [49].

Random bimodal networks were studied theoretically by Higgs and Ball [50]. In Ref. [51] Kloczkowski, Mark and Erman presented an exact analysis of bimodal phantom Gaussian networks with a regular structure; i.e. with fixed number ϕ_S of short and a fixed number ϕ_L of long chains at every ϕ-functional junction, so that $\phi = \phi_S + \phi_L$. An example of such regular bimodal network is shown in Fig. 7. It was assumed that both short and long chains have Gaussian distribution of the end-to-end vector. The phantom network model of such regular bimodal network was formulated. The analysis is similar to the analysis of unimodal networks (Eqs. (19)–(22)). The problem of fluctuations of junctions and chain dimensions is again related to finding the inverse of the connectivity matrix $\mathbf{\Gamma}$ of the network. For unimodal network all off-diagonal elements of the connectivity matrix were zero or $\gamma = -3/(2\langle r^2\rangle_0)$ depending if sites i and j were directly connected by a chain, and diagonal elements were equal $-\phi\gamma$.

Because of this the common factor γ could be removed, and the connectivity matrix was integer matrix with elements 0, -1, and ϕ. For bimodal networks the connectivity matrix is real matrix. The elements γ_{ij} are zeros if site i and j are not directly connected by a chain. If sites i and j are connected then γ_{ij} equals γ_S if the chain connecting sites i and j is a short one, and γ_L if the chain is long. The diagonal elements of the connectivity matrix are $(-\phi_S\gamma_S - \phi_L\gamma_L)$.

Similarly as for unimodal networks the inverse of the connectivity matrix for the infinite tree can be calculated

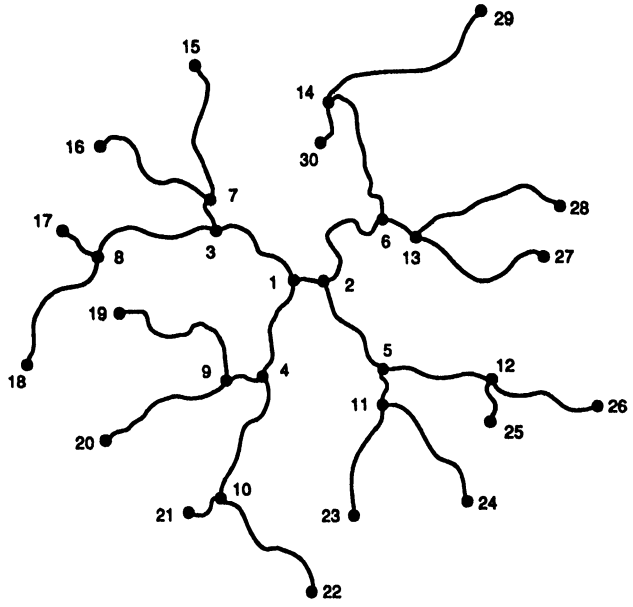

Fig. 7. Regular bimodal trifunctional network composed of four tiers. Each junction in the network is connected to one short chain and two long chains.

using recursion relations. The solution of the problem is given by a set of two equations for two unknowns A and B

$$A = \phi_L + \phi_S/\xi - \frac{(\phi_L - 1)}{A} - \frac{\phi_S}{\xi^2 B}$$
$$B = \phi_L + \phi_S/\xi - \frac{\phi_L}{A} - \frac{(\phi_S - 1)}{\xi^2 B} \tag{43}$$

where ξ $(0 < \xi < 1)$ is the ratio of the linear length of short chains to long chains. This set of equation leads to the following algebraic cubic equation for B

$$B^3(1 - \phi_L) + B^2[\xi^{-1}(\phi_S\phi_L - 2\phi_S - \phi_L + 1) + \phi_L(\phi_L - 2)] + B[\xi^{-2}(\phi_S^2 + \phi_L - 1) + \xi^{-1}(2\phi_S\phi_L + \phi_L^2 - 2\phi_L)] - \xi^{-3}(\phi_S - 1)(\phi_S + \phi_L - 1) = 0 \tag{44}$$

and A equals

$$A = \frac{B^2 - \xi^{-2} + \sqrt{(B^2 - \xi^{-2})^2 + 4B^2}}{2B} \tag{45}$$

The fluctuations of junctions in regular bimodal networks are

$$\frac{\langle(\Delta R)^2\rangle}{\langle r_L^2\rangle_0} = \frac{A}{A^2 - 1} = \frac{B}{B^2 - \xi^{-2}} \tag{46}$$

and the correlations of fluctuations of two junctions are

$$\frac{\langle(\Delta\mathbf{R})_1\cdot\Delta\mathbf{R})_2\rangle_L}{\langle\mathbf{r}_L^2\rangle_0} = \frac{1}{A^2 - 1} \tag{47}$$

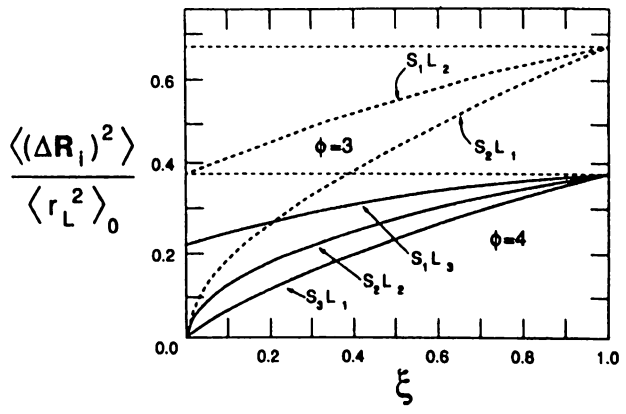

Fig. 8. Mean square fluctuations of junctions $\langle(\Delta\mathbf{R}_i)^2\rangle$ normalized by the mean square length of long chains for various regular bimodal trifunctional (dashed lines) and tetrafunctional (solid lines) networks. The subscripts m and n in the notation S_mL_n stand for the number of short chains (m) and long chains (n) connected at each junction.

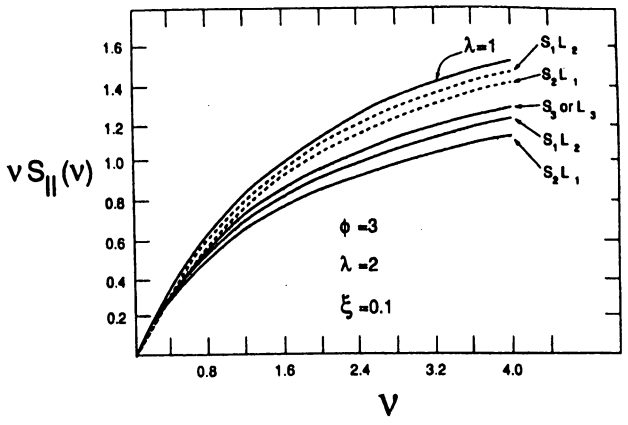

Fig. 9. Kratky plot for neutron scattering in the direction parallel to stretch from labeled short (dashed lines) and long chains (sold lines) for various regular bimodal trifunctional networks.

if junctions are connected by a long chain, and

$$\frac{\langle(\Delta\mathbf{R}_1\cdot\Delta\mathbf{R}_2)\rangle_S}{\langle\mathbf{r}_S^2\rangle_0}=\frac{1}{\xi^2B^2-1} \tag{48}$$

if junctions are connected by a short chain. Here $\langle r_L^2\rangle_0$ and $\langle r_S^2\rangle_0$ are mean square end-to-end vectors for long and short chains, respectively.

The fluctuations of junctions, and correlations of fluctuations of junctions connected by chain were calculated as a function of the ratio ξ of the length of short chains to long chains, for various regular bimodal networks. For trifunctional network ($\phi=3$) there are two types of regular bimodal networks: the first one with one short chain and two long chains at each junction (which can be abbreviated as S_1L_2 network) and the second type S_2L_1 (with two short chains and one long chain). For tetrafunctional networks ($\phi=4$) there are three types of regular bimodal networks, namely: S_1L_3, S_2L_2, and S_3L_1.

Fig. 8 shows the results obtained for various possible regular bimodal trifunctional networks. Calculations show that fluctuations of junctions increase with the length ratio ξ, and with the number of long chains ϕ_L at each junction (with functionality of the network $\phi=\phi_S+\phi_L$ kept fixed). Correlations between fluctuations of two junctions also increase with ϕ_L, but decrease with ξ for junctions connected by a short chain, and increase with ξ for junctions connected by a long chain.

The knowledge of fluctuations of junctions in the bimodal network and correlations among them enables one the calculation of fluctuations of the end-to-end vector for short chains $\langle(\Delta r_S)^2\rangle$ and long chains $\langle(\Delta r_L)^2\rangle$ in the network.

These fluctuations are

$$\frac{\langle(\Delta r_S)^2\rangle}{\langle r_S^2\rangle_0}=\frac{2}{B\xi+1} \tag{49}$$

and

$$\frac{\langle(\Delta r_L)^2\rangle}{\langle r_L^2\rangle_0}=\frac{2}{A+1} \tag{50}$$

for short and long chains respectively.

Similarly as for unimodal chains we can calculate small angle neutron scattering from a labeled chain in a regular bimodal network. The scattering form factor for the scattering in the direction parallel to the direction of stretch is:

$$S_{\|}(\mathbf{q})=2\int_o^1 d\eta(1-\eta)\exp\left\{-\upsilon\left[\lambda_{\|}^2\eta+(1-\lambda_{\|}^2)\times\left(\eta-\eta^2+\eta^2\frac{\langle(\Delta\mathbf{r})^2\rangle}{\langle r^2\rangle_0}\right)\right]\right\} \tag{51}$$

with

$$\upsilon=q^2\langle r^2\rangle_0/6 \tag{52}$$

The scattering in the direction perpendicular to the direction of stretch is obtained by replacing $\lambda_{\|}$ in Eq. (51) by $\lambda_{\perp}=1/\sqrt{\lambda_{\|}}$.

The bimodal network is composed of two types of chains, long and short ones. If short chains in the regular network are labeled then the scattering form factor for short chains is obtained from Eq. (51) with $\langle r^2\rangle_0=\langle r_S^2\rangle_0$ by replacing $\langle(\Delta r_S)^2\rangle/\langle(r_S^2)\rangle_0$ by Eq. (49) and solving Eq. (44) for B. If long chains in the regular bimodal network are labeled, the corresponding scattering form factor is obtained from Eq. (51) with $\langle r^2\rangle_0=\langle r_L^2\rangle_0$ and relative fluctuations of long chains $\langle(\Delta r_L)^2\rangle/\langle(r_L^2)\rangle_0$ given by Eq. (50).

Fig. 9 shows the results obtained for various regular trifunctional networks. Kratky plots of $\nu S(\nu)$ for scattering in the direction parallel to the direction of stretch show that the scattering form factor $S(\nu)$ increases with the number ϕ_L of long chains connected to each junction. There is no experimental SANS data for bimodal networks at the moment to compare with theoretical predictions. Bimodal

networks have been recently studied by using small angle X-ray scattering (SAXS) methods [122,123]. These experiments show that for bimodal networks exhibit scattering intensity maxima at significantly lower scattering vector **q** than unimodal networks [123].

6. Dynamic properties of Gaussian networks

The dynamics of polymer chains has been studied by many authors [52–56]. The first important paper addressing this problem was written by Rouse [52]. He assumed that linear chain in solution could be modeled as a collection of beads, connected by spring-like subchains, subject to the stochastic Brownian forces. Zimm improved later this model by adding hydrodynamic forces [54]. The Rouse–Zimm model is successful in prediction of the low frequency relaxation spectrum of chain molecules. This approach was used also to study dynamic properties of elastomeric networks.

Graessley used this method to study relaxation spectrum of tree-like micro-networks composed of few tiers [57]. He assumed that network is composed of ϕ-functional junctions which are beads subject to stochastic random forces, connected by Gaussian spring-like chains. The structure of these chains is neglected in the analysis.

Kloczkowski, Mark and Frisch [58] proposed a more detailed model of the network, with chains between ϕ-functional junctions composed also of beads (bifunctional junctions) connected by Gaussian subchains (such as a network shown in Fig. 2). This model is much more realistic and therefore gives much better insight into the dynamics of real networks.

If $(\mathbf{R}_1, \mathbf{R}_2, \ldots \mathbf{R}_N) = \{\mathbf{R}_n\}$ are positions of beads (multifunctional and bifunctional junctions) then the motion of each bead is determined by the force balance

$$\mathbf{F}_{\text{drag}} + \mathbf{F}_{\text{spring}} + \mathbf{F}_{\text{stochastic}} = 0 \tag{53}$$

which may be written as

$$-\zeta \frac{\mathrm{d}\{\mathbf{R}_n\}}{\mathrm{d}t} - K\mathbf{\Gamma}\{\mathbf{R}_n\} + \{\mathbf{f}_n\} = 0 \tag{54}$$

Here ζ is the frictional coefficient, taken to be the same for each bead regardless of its functionality, K is the spring constant defined by:

$$K = 3k_{\mathrm{B}}T/\langle r^2\rangle_0 \tag{55}$$

where $\langle r^2\rangle_0$ is the mean square end-to-end distance for the unstretched subchain, k_{B} the Boltzman constant, T the temperature, $\mathbf{\Gamma}$ the connectivity matrix and $\{\mathbf{f}_n\}$ a set of random, stochastic forces acting on beads located at $\{\mathbf{R}_n\}$. The connectivity matrix has very regular structure with elements contributed from multifunctional junctions and from bifunctional junctions. Such matrices were studied in detail in Ref. [37].

The eigenvalues $\lambda_i\ (i = 1, 2, \ldots N)$ of the connectivity matrix $\mathbf{\Gamma}$ are solutions of the characteristic (secular) equation

$$\det(\mathbf{\Gamma} - \lambda \mathbf{I}_N) = 0 \tag{56}$$

where $\mathbf{I}_N$ is identity matrix of order N. Each eigenvalue λ_i is associated with the relaxation time of the ith model

$$\tau_i = \frac{\tau_0}{\lambda_i} \qquad i = 1, 2, \ldots N \tag{57}$$

Here τ_0 is the primary relaxation time of a single unattached subchain

$$\tau_0 = \frac{\zeta}{K} \tag{58}$$

determined by the frictional coefficient ζ of the beads and the spring constant K (given by Eq. (55) of a subchain. For a very large system in the limit $N \rightarrow \infty$ the distribution of eigenvalues $\lambda(\xi)$ and relaxation times $\tau(\xi)$ is described by continuous variable ξ, and the relaxation spectrum $H(\tau)$ is defined by:

$$H(\tau) = -\upsilon k_{\mathrm{B}}T \frac{\mathrm{d}\xi}{\mathrm{d}\ln\tau} \tag{59}$$

where υ is the number of beads per unit volume. The relaxation modulus $G(t)$ is defined as an integral of the relaxation spectrum $H(\tau)$

$$G(t) = G_{\mathrm{e}} + \int_{-\infty}^{\infty} H(\tau)\, \mathrm{e}^{-t/\tau}\, \mathrm{d}\ln\tau \tag{60}$$

or alternatively

$$G(t) = G_{\mathrm{e}} + \upsilon k_{\mathrm{B}}T \sum_{i=1}^{N} \exp\left(-\frac{\lambda_i t}{\tau_0}\right) \tag{61}$$

where G_{e} is the equilibrium shear modulus of the network. The main problem in calculating the relaxation spectrum $H(\tau)$ and relaxation modulus $G(t)$ is to solve the eigenvalue problem. The characteristic equation for eigenvalues of the connectivity matrix $\mathbf{\Gamma}$ is given by product of determinants $\det(\mathbf{\Gamma}_j - \lambda \mathbf{I}_{N_j})$ of submatrices $\mathbf{\Gamma}_j$ corresponding to subsequent tiers $(1 \le j \le J)$

$$\begin{aligned}\det(\mathbf{\Gamma} - \lambda \mathbf{I}_N) &= \prod_{j=1}^{J} \det(\mathbf{\Gamma}_j - \lambda \mathbf{I}_{N_j}) \\ &= [a_1 U_{n-1}(x) - U_{n-2}(x)]^{m_J} [a_2 U_{n-1}(x) - U_{n-2}(x)]^{m_{J-1}} \times \ldots \\ &\quad \times [a_{J-1} U_{n-1}(x) - U_{n-2}(x)]^{m_2} \{a_J^2 U_{n-1}(x) - 2a_J U_{n-2}(x) \\ &\quad + U_{n-3}(x)\} \\ &= 0\end{aligned} \tag{62}$$

with coefficients a_k satisfying the recurrence relation

$$a_k = \phi - \lambda - \frac{(\phi - 1)[a_{k-1} U_{n-2}(x) - U_{n-3}(x)]}{a_{k-1} U_{n-1}(x) - U_{n-2}(x)} \tag{63}$$

and $U_k(x)$ denoting the Chebyshev polynomials of the

second kind $U_n(x) = \sin[(n+1)\ \ x]/\sin[\arccos x]$. The final equation for eigenvalues has the following form:

$$U_k\left[\frac{U_n\left(1-\frac{\lambda}{2}\right)+(\phi-2)U_{n-1}\left(1-\frac{\lambda}{2}\right)-(\phi-1)U_{n-2}\left(1-\frac{\lambda}{2}\right)}{2\sqrt{\phi-1}}\right]$$

$$+\sqrt{\phi-1}U_{n-2}\left(1-\frac{\lambda}{2}\right)U_{k-1}\left[\frac{U_n\left(1-\frac{\lambda}{2}\right)+(\phi-2)U_{n-1}\left(1-\frac{\lambda}{2}\right)-(\phi-1)U_{n-2}\left(1-\frac{\lambda}{2}\right)}{2\sqrt{\phi-1}}\right]=0 \qquad (64)$$

for $1 \le k \le J-1$. Eq. (64) is a highly complicated double Chebyshev polynomial of order kn in λ. It can be shown that when the number of tiers of the tree goes to infinity the asymptotic solution of the problem is

$$U_n\left(1-\frac{\lambda}{2}\right)+(\phi-2)U_{n-1}\left(1-\frac{\lambda}{2}\right)-(\phi-1)U_{n-2}\left(1-\frac{\lambda}{2}\right)$$
$$=2\sqrt{\phi-1}\cos\frac{\pi r}{k+1} \qquad (65)$$

with $r = 1, 2 \ldots k$. Eq. (65) represents the simplified analytical solution of the eigenvalue problem for the network. Instead of a polynomial of the order nk in λ (Eq. (64)) we have a set of k polynomial equations of order n. Eq. (65) can be solved analytically for $n = 1$ or 2, and numerically for the larger number of chain beads n.

The relaxation spectrum of the network is given by equation:

$$H(\tau) = \frac{\upsilon k_B T \tau_0}{2\pi\tau} \times \frac{[U'_n(x)+(\phi-2)U'_{n-1}(x)-(\phi-1)U'_{n-2}(x)]}{\sqrt{4(\phi-1)-[U_n(x)+(\phi-2)U_{n-1}(x)-(\phi-1)U_{n-2}(x)]^2}} \qquad (66)$$

where

$$U'_n(x) \equiv \frac{d}{dx}U_n(x) = \frac{1}{x^2-1}[(n+2)T_{n+1}(x) - U_{n+1}(x)] \qquad (67)$$

and

$$x = 1 - \frac{\lambda}{2} = 1 - \frac{\tau_0}{2\tau}$$

Here $T_n(x)$ denotes the Chebyshev polynomial of the first kind $T_n(x) = \cos(n \arccos x)$.

It can be shown that the relaxation spectrum $H(\tau)$ satisfies some mathematical inequalities, which give the band structure of the spectrum. The complexity of this band structure increases with the number of beads n of network chains. This is shown in Fig. 10.

The relaxation modulus $G(t)$ of the network is

$$G(t) = G_e + \frac{\upsilon k_B T}{\pi} e^{-2t/\tau_0} \int_{-\infty}^{1} dx \times \frac{e^{2tx/\tau_0}[U'_n(x)+(\phi-2)U'_{n-1}(x)-(\phi-1)U'_{n-2}(x)]}{\sqrt{4(\phi-1)-[U_n(x)+(\phi-2)U_{n-1}(x)-(\phi-1)U_{n-2}(x)]^2}} \qquad (68)$$

where G_e is the equilibrium shear modulus of the network, and the integral is defined only for bands with positive slopes.

The inclusion of bifunctional junctions (beads) along the chain considerably broadens the relaxation spectrum of the network and gives a more realistic description of the spectrum at shorter times. The new theory has been very useful in interpretation of recent experimental data [59,60,151].

A new theory relaxation spectra and viscoelastic dynamic properties of polymer networks with interchain friction and long-range hydrodynamic interactions have been recently proposed by Gotlib and Gurtovenko [108–110]. These authors in collaboration with Kilian extended the theoretical treatment to heterogenous polymer networks [111,112].

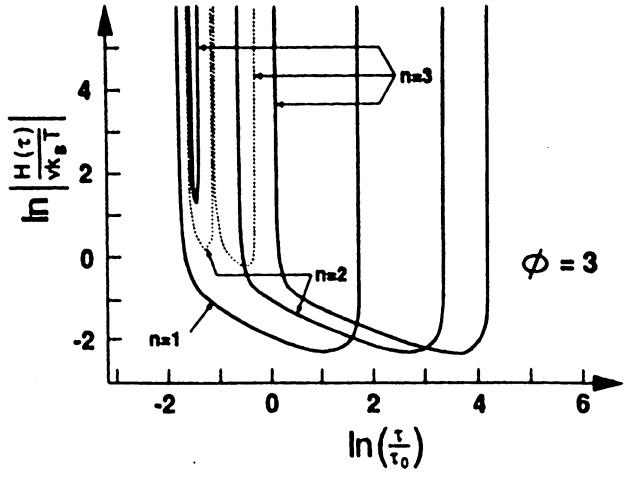

Fig. 10. Relaxation spectra for trifunctional network for different number n of subchains between junctions. The case $n = 1$ corresponds to Graessley spectrum. Dotted lines correspond to unphysical negative $H(\tau)$.

7. Effects of constraints along polymer chains

Real elastomeric network exhibit properties that fall between those of the affine and phantom models, discussed in Section 1. The first theoretical model of real polymer networks was developed by Flory in 1976 [30]. He developed the constrained junction model of rubber elasticity, discussed briefly earlier. In real networks the excluded volume and entanglements effect the elastic behavior of polymer chains. A parameter which measures the effect of chain constraints is the degree of chain interpenetration in the network, defined as the average number of spatially neighboring junctions within the domain of fluctuations of a given junction in the network.

In the constrained junction network model a given junction is assumed to be under the joint action of the phantom network and the constraint domains. The effect of constraining fluctuations of junctions is measured by the parameter κ in the Flory theory defined by Eq. (13). The elastic free energy is given by Eq. (14) with variables B_t and D_t (for Cartesian components $t = x, y, z$) defined by Eqs. (15) and (16).

Experimental data for rubberlike materials usually are shown as Mooney–Rivlin plots of the reduced force $[f^*]$ as a function of the inverse of elongation α^{-1}. The reduced force (or a modulus) $[f^*]$ is defined as:

$$[f^*] = \frac{f v_2^{1/3}}{A_d(\alpha - \alpha^{-2})} \tag{69}$$

where f is force, where A_d is the cross-sectional area of the sample in the dry state, and v_2 is the volume fractions of the polymer in the network in the final state. The reduced force $[f^*]$ at uniaxial deformation for the constrained junction theory of Flory is

$$[f^*] = [f^*]_{ph} = \left[1 + \frac{2}{\phi - 2} \frac{[\alpha K(\lambda_1^2) - \alpha^{-2} K(\lambda_2^2)]}{\alpha - \alpha^{-2}} \right] \tag{70}$$

where $\lambda_1 = \lambda$ and $\lambda_2 = \lambda^{-1/2}$, $[f^*]_{ph}$ is the phantom modulus

$$[f^*]_{ph} = \frac{\left(1 - \frac{2}{\phi}\right) \nu k T v_{2c}^{2/3}}{V_d} \tag{71}$$

where $v_{2c} = V_d/V_0$ and V_d and V_0 are volume of the network in the dry state and in the reference state, respectively.

The function $K(\lambda^2)$ is defined as:

$$K(\lambda^2) = \frac{B\dot{B}}{B+1} + \frac{D\dot{D}}{D+1} \tag{72}$$

with $B(\lambda^2)$ and $D(\lambda^2)$ given by Eqs. (15) and (16) and

$$\dot{B} \equiv \frac{\partial B}{\partial \lambda^2} = B\left[\frac{1}{\lambda^2 - 1} - \frac{2}{\lambda^2 + \kappa} \right] \tag{73}$$

and

$$\dot{D} \equiv \frac{\partial D}{\partial \lambda^2} = \frac{1}{\kappa}(\lambda^2 B + B) \tag{74}$$

The reduced force $[f^*]$ in the constrained junction theory of Flory lies always between the modulus of the affine network $[f^*]_{aff}$ and the modulus of the phantom network $[f^*]_{ph}$ (given by Eq. (71), irrespective of the elongation. In the limit $\kappa = 0$ Eq. (70) gives the phantom modulus, while in the limit $\kappa = \infty$ it reaches the affine modulus.

Erman and Monnerie [61,62] used Flory's idea of constraints effecting fluctuations in real networks, relative to fluctuations in phantom networks, but with constraints effecting fluctuations of the centers of masses of chains, instead of junctions. The elastic free energy in their constrained chain theory is given (similarly as in the constrained junction theory) as a sum of free energy of the phantom network and the contribution due to constraints on chains. The later part has identical mathematical form as in the constrained junction model

$$\Delta A_c = \frac{1}{2} \nu k T \sum_{t=x,y,z} [B_t + D_t - \ln(B_t + 1) - \ln(D_t + 1)] \tag{75}$$

and only B_t and D_t are defined differently, namely

$$B_t = \frac{h \kappa_G (1 - \Phi)(\lambda_t^2 - 1)}{(\lambda_t^2 + h)^2} \tag{76}$$

and

$$D_t = \frac{\lambda_t^2 B_t}{h} \tag{77}$$

where the parameter h is a function of the macroscopic deformation tensor $\boldsymbol{\lambda}$

$$h(\lambda_t) = \kappa_G[1 + (\lambda_t^2 - 1)\Phi] \tag{78}$$

Here the parameter Φ is given by the formula

$$\Phi = \left(1 - \frac{2}{\phi}\right)^2 \left(\frac{1}{3} + \frac{2}{3n}\right) \tag{79}$$

The parameter κ_G is a measure of the strength of constraints effecting the fluctuations of the center of mass of the chain in the phantom network, and is defined similarly to the parameter κ (Eq. (13)) in the constrained junction theory as a ratio of fluctuations of the center of mass of the chain to the domain size of the constraint affecting fluctuations of the center of mass of the chain.

The constrained chain theory of Erman and Monnerie leads to the following expression for the reduced force (modulus)

$$[f^*] = [f^*]_{ph} \left[1 + \frac{\phi}{\phi - 2} \frac{[\alpha K(\lambda_1^2) - \alpha^{-2} K(\lambda_2^2)]}{\alpha - \alpha^{-2}} \right] \tag{80}$$

where $\lambda_1 = \lambda$ and $\lambda_2 = \lambda^{-1/2}$, $[f^*]_{ph}$ is the phantom modulus, the function $K(\lambda^2)$ is defined as previously by Eq. (72),

but with $B(\lambda^2)$ and $D(\lambda^2)$ now given by Eqs. (76) and (77). The reduced force in the constrained chain model converges to the phantom modulus in the limit $\kappa_G = 0$, but for sufficiently large value of κ_G exceeds the affine modulus.

In real networks constraints do not affect only fluctuations of junctions, or fluctuations of the center of mass of the chain. The constraints are distributed uniformly within the network and they affect fluctuations of both junctions, and all chain segments. Kloczkowski, Mark and Erman [63] formulated the new theory which addresses these problems. The constraints in this theory which is called 'diffused-constraint', are applied continuously along chains.

The probability of the fluctuation $\Delta\mathbf{R}_i$ of the point i (located at the fractional distance θ from one of chain ends) from its mean position in the phantom network is

$$P(\Delta\mathbf{R}_i) = C\exp\left[-\frac{\gamma}{\frac{\phi-1}{\phi(\phi-2)}+\left(1-\frac{2}{\phi}\right)\theta(1-\theta)}(\Delta\mathbf{R}_i)^2\right] \tag{81}$$

with

$$\gamma = \frac{3}{2\langle r^2\rangle_0} \tag{82}$$

where C is the normalization constant and θ is the fractional postion of point i along the chain (see Eq. (27)). If the point i of the chain is under the joint action of the phantom network and the constraints then following the treatment of Flory the joint probability of having point i at $\delta\mathbf{R}_i$ in the real network is

$$P(\delta\mathbf{R}_i) = CP(\Delta\mathbf{s})P(\Delta\mathbf{R}_i) \tag{83}$$

where $P(\Delta\mathbf{s})$ is the distribution of constraints which was assumed by Flory to be Gaussian and affine under deformation. The distribution $P(\Delta\mathbf{s})$ is independent of the position of the center of constraints, if on average constraints are uniformly distributed inside the network. We assume that the Gaussian parameter s_0 of distribution $P(\Delta\mathbf{s})$ is the same for all points i along the chain, and is the same as in the constrained junction theory of Flory. The probability of the fluctuation of the point i along the chain from its mean position in phantom network $\bar{A}_i$ in the presence of constraints $P^*(\Delta\mathbf{R}_i)$ is given by the convolution

$$P^*(\Delta\mathbf{R}_i) = P(\delta\mathbf{R}_i)^*\Theta(\Delta\bar{\mathbf{R}}) \tag{84}$$

where $\Theta(\Delta\bar{\mathbf{R}})$ is a Gaussian distribution independent of deformation.

Following Flory's arguments it may be shown that the distribution $P^*(\Delta X_i)$ for the x-component of the point i on the chain in the real network in the presence of constraints is (with similar equations for y and z components):

$$P^*(\Delta X_i) = C\exp\left[-\frac{\alpha'}{1+\frac{\kappa^2(\lambda_x^2-1)}{(\lambda_x^2+\kappa)^2}}(\Delta X_i)^2\right] \tag{85}$$

with

$$\alpha' = \frac{\gamma}{\frac{\phi-1}{\phi(\phi-2)}+\left(1-\frac{2}{\phi}\right)\theta(1-\theta)} \tag{86}$$

The parameter κ in Eq. (85) is now point i-dependent function

$$\kappa(\theta) = \frac{\sigma_0}{\alpha'} = \frac{\sigma_0}{\gamma}\left[\frac{\phi-1}{\phi(\phi-2)}+\left(1-\frac{2}{\phi}\right)\theta(1-\theta)\right] \tag{87}$$

Following the arguments used by Flory in the constrained junction theory the elastic free energy of the constraints effecting fluctuations of the ith segment of network chains is

$$\Delta A_c(\theta) = \frac{1}{2}\nu kT\sum_{t=x,y,z}[B_t(\theta)+D_t(\theta)-\ln[B_t(\theta)+1] - \ln[D_t(\theta)+1]] \tag{88}$$

with

$$B_t(\theta) = \frac{\kappa^2(\theta)\left(\lambda_t^2-1\right)}{\left[\lambda_t^2+\kappa(\theta)\right]^2} \tag{89}$$

and

$$D_t(\theta) = \frac{B_t(\theta)\lambda_t^2}{\kappa(\theta)} \tag{90}$$

Because the constraints are affecting fluctuations of all points along the chain, the averaging of the free elastic energy of constraints is performed over all segments of the chain which leads to:

$$\Delta A_c = \frac{1}{2}\nu kT\sum_{t=x,y,z}\int_0^1 W(\theta)[B_t(\theta)+D_t(\theta)-ln[B_t(\theta)+1] - \ln[D_t(\theta)+1]]d\theta \tag{91}$$

Here $W(\theta)$ is the distribution of constraints among different points along the chain. If this distribution is uniform then $W(\theta) = 1$ inside the integrand of Eq. (91).

In the case when constraints are assumed to effect only fluctuations of junctions

$$W(\theta) = \delta(\theta)+\delta(\theta-1) \tag{92}$$

where δ denotes the Dirac δ-function. Also, because each junction is shared by ϕ chains, ν in Eq. (91) should be replaced by $2\nu/\phi = \mu$ and the elastic free energy of constraints of the Flory theory is recovered.

If constraints are assumed to effect the fluctuations of the

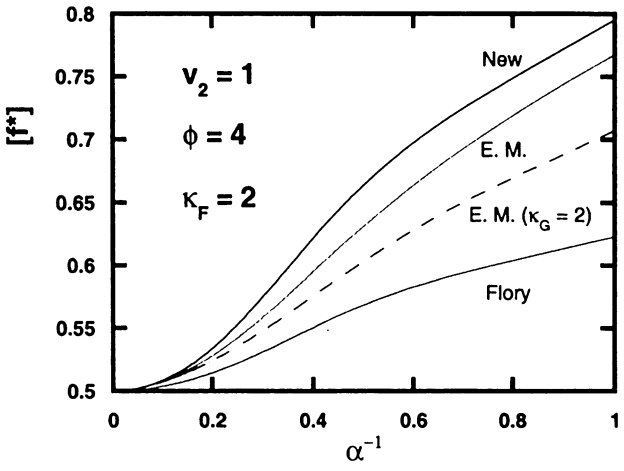

Fig. 11. Comparison of various constraint theories of rubber elasticity. The modulus $[f^*]$ (normalized by $\nu kT\nu_{2c}^{2/3}/V_d$ is plotted as a function of the inverse elongation α^{-1} for dry ($\nu_2 = 1$) tetrafunctional network ($\phi = 4$) for the Erman–Monnerie theory (E.M.), the Flory theory and the present theory (new) calculated for $\kappa_F = 2$, and additionally for $\kappa_G = 2$ for the Erman–Monnerie theory (dashed line).

midpoint of the chain only then

$$W(\theta) = \delta(\theta - 1/2) \tag{93}$$

which leads to an expression similar (but not identical) to the elastic free energy of constraints in the Erman–Monnerie theory [61,62]. The diffused-constraint theory does not reduce identically to the Erman–Monnerie constrained chain theory, because instead of the deformation-independent fluctuations of the midpoint of the chain they studied the deformation-dependent fluctuations of the center of mass of the chain.

The reduced force (modulus) in the diffused-constraints theory is given by the integral

$$[f^*] = [f^*]_{ph}\left[1 + \frac{\phi}{\phi - 2}\frac{\left[\alpha K\left(\lambda_1^2\right) - \alpha^{-2}K\left(\lambda_2^2\right)\right]}{\alpha - \alpha^{-2}}\mathrm{d}\theta\right] \tag{94}$$

Fig. 11 compares the results of the diffused-constraint theory with other theories. The calculated modulus is larger than the modulus obtained from the constrained chain theory, and larger than the modulus obtained from the Flory constrained junction theory. Because of this the diffused-constraint theory fits well experimental data for relatively low values of the parameter κ, while Erman–Monnerie and Flory theories require much larger values of κ. In a recent paper Urayama, Kawamura and Kohjiya [154] tested and compared various most recent theories of the rubber elasticity, similarly as Gotlieb and Gaylord tested 'older' theories in the 1980s [155]. Urayama and coworkers compared Kloczkowski, Erman and Mark diffused-constraints model with Edwards–Vilgis slip-link theory [150] and with three most recent tube models: Gaylord and Douglas model [140,141], Heinrich, Straube and Helmis model [120] and Rubinstein and Panyukov model [142].

The predictions of all these models were fitted to experimental data. Each of these models has different number of adjustable parameters. Kloczkowski–Erman–Mark model has only one parameter κ_F measuring the severity of entanglements. Gaylord–Douglas and Rubinstein–Panyukov theories also have one adjustable parameter, while Heinrich–Straube–Helmis model has two adjustable parameters and Edwards and Vilgis model have three adjustable parameters. The results of Urayama and coworkers show that the diffused-constraints theory is more successful in reproducing stress–strain data than all tube models, the only deficiency of this theory comes from the underestimation of the equilibrium modulus G_0, because trapped entanglements are neglected in this theory. The Edwards–Vilgis model is the most successful but at the cost of having two additional adjustable parameters. The slight modification the 'diffused constraint' theory to include additional adjustable parameter for fitting the equilibrium modulus could probably lead to the best performance of this theory in comparison with all other models.

The diffused-constraint theory was also applied to the theoretical analysis of strain birefringence in deformed polymer networks [64]. The birefringence of polarized light, i.e. the dependence of the refractive index on the direction of light polarization is observed in anisotropic media. In the isotropic medium the refractive index does not depend on the direction of the light polarization. The birefringence is observed in stretched polymer samples. The refractive index in the direction parallel to the direction of stretch differs from the refractive index in the perpendicular direction, and the birefringence is related to the degree of molecular order of the sample [65–69].

The stress birefringence is a simple and useful method to study the relationship between the macroscopic deformation of the network and the corresponding alignment of chains at the molecular level, and is an excellent method for testing various molecular theories of rubberlike elasticity.

The difference between polarizabilities in direction x and y is related to the molecular deformation tensor

$$\bar{\alpha}_{xx} - \bar{\alpha}_{yy} = \frac{\Gamma_2}{3}\left(\Lambda_x^2 - \Lambda_y^2\right) \tag{95}$$

The molecular deformation tensor $\mathbf{\Lambda}$ is defined for different components of the end-to-end vector as

$$\mathbf{\Lambda}_t^2 = \frac{\langle t^2\rangle}{\langle t^2\rangle_0} \quad (t = x, y, z) \tag{96}$$

which may differ from the macroscopic deformation tensor $\boldsymbol{\lambda}$, and Γ_2 is a constant. In the case of the affine model of the network proposed by Kuhn the molecular deformation tensor $\boldsymbol{\lambda}$ is identical with the macroscopic deformation tensor $\mathbf{\Lambda}$. For the ϕ-functional phantom model of the

network deformation the relation between tensors $\mathbf{\Lambda}$ an $\boldsymbol{\lambda}$ is

$$\Lambda_{t,\mathrm{ph}}^2 = \left(1 - \frac{2}{\varphi}\right)\lambda_t^2 + \frac{2}{\varphi} \quad (t = x, y, z) \tag{97}$$

The molecular deformation tensor in the constrained junction theory [30] is

$$\Lambda_t^2 = \left(1 - \frac{2}{\varphi}\right)\lambda_t^2 + \frac{2}{\varphi}(1 + B_t) \quad (t = x, y, z) \tag{98}$$

where B_t is defined by Eq. (15). However in addition to the molecular deformation tensor $\mathbf{\Lambda}^2$, there is also the domain deformation tensor $\mathbf{\Theta}^2$ defined as

$$\Theta_t^2 = 1 + D_t \tag{99}$$

(with D_t given by Eq. (16) and the total effective microscopic tensor is a sum of $\mathbf{\Lambda}^2$ and $(\mathbf{\Theta}^2 - 1)$ scaled by a factor b $(0 < b < 1)$

$$\Lambda_{t,\mathrm{eff}}^2 = \left(1 - \frac{2}{\varphi}\right)\lambda_t^2 + \frac{2}{\varphi}(1 + B_t + bD_t) \tag{100}$$

The free energy of constraints in the Erman–Monnerie theory of constrained chain [61,62] is proportional to the number of chains μ. This leads to a slightly different expression for the molecular deformation tensor than Eq. (100), namely

$$\Lambda_{t,\mathrm{eff}}^2 = \left(1 - \frac{2}{\varphi}\right)\lambda_t^2 + \frac{2}{\varphi} + B_t + bD_t \tag{101}$$

with B_t and D_t defined by Eqs. (76) and (77).

The effective deformation tensor in the diffused-constraint theory is given by the following formula:

$$\Lambda_{t,\mathrm{eff}^2} = \left(1 - \frac{2}{\varphi}\right)\lambda_t^2 + \frac{2}{\varphi} + \int_0^1 \mathrm{d}\theta W(\theta)[B_t(\theta) + bD_t(\theta)] \tag{102}$$

with $B_t(\theta)$ and $D_t(\theta)$ defined by Eqs. (89) and (90). If constraints are distributed uniformly along the chain $W(\theta) = 1$ then the reduced birefringence is given by the formula:

$$[\Delta\tilde{n}] = \frac{\xi}{V_0} kTC\left[1 + \frac{\phi}{\phi - 2}\left(\frac{V_0}{V}\right)^{2/3} \times \frac{\int_0^1 \mathrm{d}\theta\, W(\theta)[B_x(\theta) - B_y(\theta) + b[D_x(\theta) - D_y(\theta)]]}{\alpha^2 - \alpha^{-1}}\right] \tag{103}$$

where ξ is the cycle rank of the network, and C is the stress-optical coefficient.

The numerical calculations show that the reduced birefringence for the diffused-constraint theory is larger than the birefringence for the constrained chain and constrained junction model. This is shown in Fig. 12. Similarly as for the modulus we can use much smaller (and more realistic)

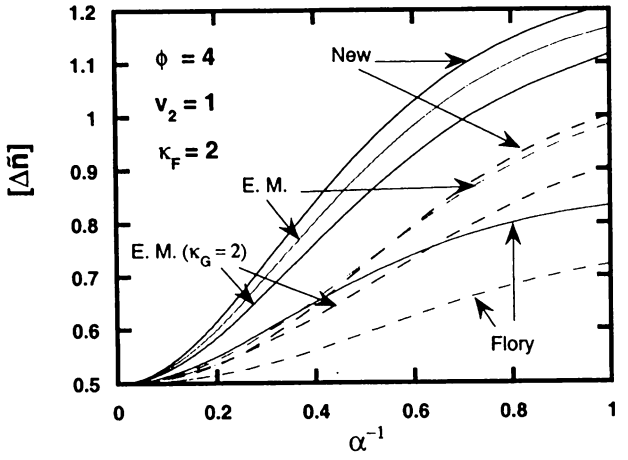

Fig. 12. Comparison of the reduced birefringence as a function of the inverse elongation for various models of the rubberlike elasticity: Flory constrained junction theory, Erman–Monnerie theory (E.M.) and the diffused-constraint theory (New). The calculations were performed for dry tetrafunctional network with $\kappa_F = 2$. The solid lines correspond to the scaling factory $b = 1$, and the dashed lines to $b = 0$.

values of the parameter κ to fit experimental data, then κ in the constrained junction and the constrained chain models.

8. Segmental orientation and isotropic–nematic phase transitions in deformed rubberlike networks of semi-rigid chains

Segmental orientation (or molecular orientation) denotes the anisotropic distribution of orientations of chain segments in space. Segmental orientation in elastomeric networks can be obtained under uniaxial deformation of the sample. Segmental orientation in stretched networks can be measured by the quantity

$$S_0 = \frac{1}{5m}(\lambda^2 - \lambda^{-1}) \tag{104}$$

The orientation function S_0 is given by the average value of the second Legendre polynomial $\langle P_2(\cos\psi)\rangle$ of the cosine of the angle ψ between the direction of polymer segment and the direction stretch. Here m is the number of Kuhn segments in a network chain, and λ is the extension ratio defined as the ratio of the deformed length of a sample to that in the reference state. Eq. (104) represents the leading term of a more general expression based on the inverse Langevin function [67]. The first theory of segmental orientation was proposed by Kuhn and Grün [70] and was based on the assumption that the chain segments do not interact with their neighbors, i.e. intermolecular effects on segmental orientation are absent and the chains are phantom-like. The theory of Kuhn and Grün is frequently referred to in the literature as 'gaslike', because of the phantom-like nature of polymer chains.

An improvement of this theory by taking into account

intermolecular interactions was proposed by Di Marzio [71], and later by Tanaka and Allen [72] and other authors [73,74]. The theoretical treatment of the excluded volume of polymer chains in these papers was possible by using lattice representations of polymer chains. Each segment was represented on a lattice as a lattice point, and one site can not accommodate more than one segment, which models the excluded volume condition for real chains. These improved theories are often called 'liquid-like'.

Polymeric materials with sufficiently stiff segments show liquid-crystalline behavior. There is a possibility of the nematic–isotropic phase transition upon stretching the sample.

Erman, Bahar, Kloczkowski and Mark [75] developed a theory of segmental orientation, which (additionally to the excluded volume) takes directly into account chain stiffness, and which predicts liquid-crystalline behavior and nematic–isotropic phase transtition in stretched polymer networks. For this purpose the lattice theory of Flory for chains with freely jointed rodlike segments was adapted [76–78]. The length-to-width ratio x of each Kuhn segment of a chain is a measure of chain stiffness in the theory. Each chain is composed of m Kuhn segments with length-to-width ratio x. The system of n_2 polymer and n_1 solvent molecules in a lattice consisting of n_0 sites was considered, with the respective volume fractions of polymer and solvent:

$$v_2 = \mathrm{mxn_2/n_0} \qquad v_1 = n_1/n_0 \tag{105}$$

In the Flory lattice treatment of polymer chains the orientation of each rod-like segment is given by disorientation index y_k

$$y_k = x \sin\psi_k(|\cos\phi_k| + |\sin\phi_k|) \tag{106}$$

where ψ_k and ϕ_k are Euler angles of a given segment. It is then possible to derive the combinatorial part of partition function Z_{comb}

$$\begin{aligned}-\ln Z_{\mathrm{comb}} = {} & n_1 \ln v_1 + n_2 \ln(v_2/mx) \\ & - (n_1 + n_2 m\bar{y}) \ln[1 - v_2(1 - \bar{y}/x)] \\ & + n_2(m\bar{y} - 1) - n_2(m - 1)\ln(z - 1)\end{aligned} \tag{107}$$

and the oriental part of partition function Z_{orient}

$$-\ln Z_{\mathrm{orient}} = n_2 \ln n_2 - n_2 - n_2 m \ln m + \sum_{j=1}^{n_2} \sum_{k} n_{j,k} \ln \frac{n_{j,k}}{\omega_k} \tag{108}$$

and the free energy of mixing the system, which is

$$\Delta A_m = -k_{\mathrm{B}} T \ln(Z_{\mathrm{comb}} Z_{\mathrm{orient}}) \tag{109}$$

Here $n_{j,k}$ is the number of segments of the j-th chain with orientation within the k-th fractional range of solid angle ω_k.

To obtain the orientational distribution of segments under deformation the free energy ΔA_m was minimized with respect to $n_{j,k}$ for a chain with the fixed end-to-end vector was done by the use of Lagrange multipliers method. It was also assumed that the end-to-end vector transforms affinely under deformation. This leads to the system of three nonlinear equations for $\bar{y}$ and two unknown Lagrange multipliers β, γ with double integrals over angles ϕ, ψ

$$\frac{\bar{y}}{x} = \frac{\int_0^{2\pi} \mathrm{d}\phi \int_0^{\pi} \mathrm{d}\psi \sin\psi[|\cos\phi| + |\sin\phi|] f(\phi,\psi)}{\int_0^{2\pi} \mathrm{d}\phi \int_0^{\pi} \mathrm{d}\psi f(\phi,\ \psi)} \tag{110a}$$

$$\frac{\lambda}{(3m)^{1/2}} = \frac{\int_0^{2\pi} \mathrm{d}\phi \int_0^{\pi} \mathrm{d}\psi \cos\psi f(\phi,\psi)}{\int_0^{2\pi} \mathrm{d}\phi \int_0^{\pi} \mathrm{d}\psi f(\phi,\psi)} \tag{110b}$$

$$\frac{1}{(3m\lambda v_2)^{1/2}} = \frac{\int_0^{2\pi} \mathrm{d}\phi \int_0^{\pi} \mathrm{d}\psi \sin\psi\cos\psi f(\phi,\psi)}{\int_0^{2\pi} \mathrm{d}\phi \int_0^{\pi} \mathrm{d}\psi f(\phi,\psi)} \tag{110c}$$

Here $f(\phi,\psi)$ is the orientional distribution function

$$\begin{aligned}f(\phi,\psi) = \sin\psi \exp[-ax \sin\psi[|\cos\phi| + |\sin\phi| \\ + \beta\cos\psi + \gamma \sin\psi(\cos\phi + \sin\phi)]]\end{aligned} \tag{111}$$

and the parameter a is

$$a = -\ln[1 - v_2(1 - \bar{y}/x)] \tag{112}$$

The orientation function is then

$$S = \langle P_2(\cos\psi)\rangle = \int_0^{2\pi} \mathrm{d}\phi \int_0^{\pi} \mathrm{d}\psi \left(\frac{3}{2}\cos^2\psi - \frac{1}{2}\right) \tag{113}$$

It is possible to linearize the set of nonlinear equations (Eqs. (110a)–(110c)). The solution of the linearized system of equations leads to a critical value of the length-to-width ratio of Kuhn segments

$$x_a = \frac{3}{(4/\pi) - 1} = 10.98 \tag{114}$$

For x larger than 10.98 the system is always anisotropic. The exact relation between true stress σ

$$\sigma = \frac{1}{V}\lambda\left(\frac{\partial \Delta A_m}{\partial\lambda}\right)_{T,V,n_1,n_2,n_{(j,k)\mathrm{eq}}} \tag{115}$$

and strain in deformed networks of semi-rigid chains was also derived [79]. The final expression is

$$\sigma = \frac{k_{\mathrm{B}}T}{V} n_2 \sqrt{m/3\lambda}[\beta - \gamma/\sqrt{v_2\lambda^3}] \tag{116}$$

with coefficients β and γ given by Eqs. (110a)–(110c). The linearized version of this equation

$$\sigma = \frac{k_{\mathrm{B}}T}{V} n_2(\lambda^2 - 1/\lambda v_2) \tag{117}$$

does not show the dependence of stress on the rigidity of

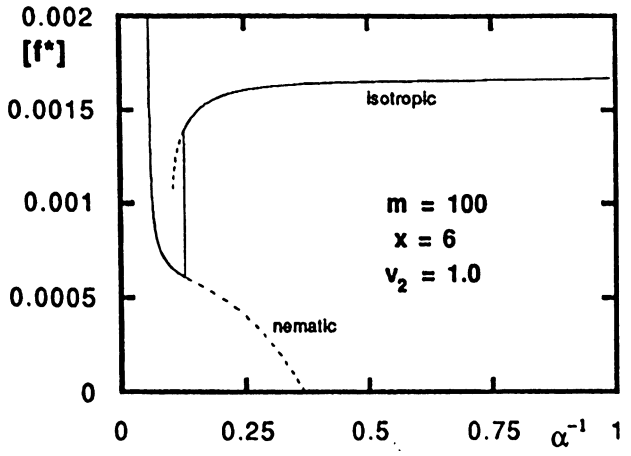

Fig. 13. The reduced stress $[f^*]$ as a function of α^{-1} for a phase transitions at constant length.

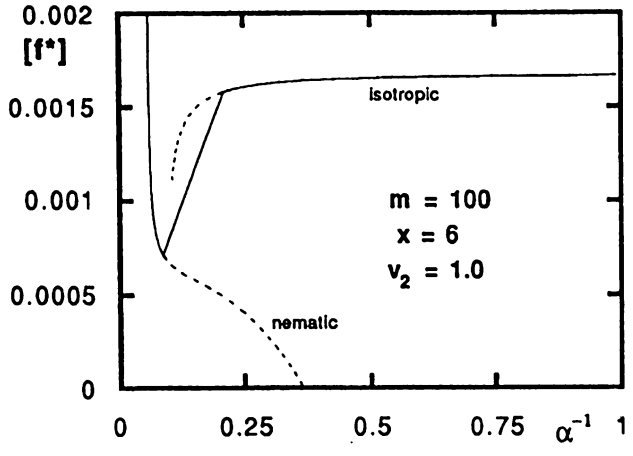

Fig. 14. The reduced stress $[f^*]$ as a function of α^{-1} for a phase transitions at constant force.

segments measured by the parameter x. The numerical solution of the system of nonlinear equations shows many interesting features. The most interesting is the possibility of isotropic–nematic equilibria in deformed polymer networks. The thermodynamic parameters which can be easily controlled during the phase transition are either the length of the sample measured by the extension ratio λ, or the applied force f.

The isotropic–nematic transition at constant length occurs when the free energies of the nematic and the isotropic phase are equal.

$$\Delta A_m(\text{isotropic}) = \Delta A_m(\text{nematic}) \tag{118}$$

The phase with the lowest free energy prevails. For the athermal system the isotrophic phase is stable at low axial ratios x and at low concentrations of semi-rigid chains v_2. For sufficiently high axial ratios and high values of v_2 the nematic solution has lower free energy than the isotropic one. There is a critical value of the axial ratio x_{crit} (given by Eq. (114)) below which the nematic solution never exists regardless of the deformation λ. This is shown in Fig. 13.

We may also study the phase transition at constant force f, when the length L of the sample changes. The proper free energy ΔG_m for studying the phase transitions at constant force f is

$$\Delta G_m = \Delta A_m - fL \tag{119}$$

The phase transition at constant force occurs when the free energies ΔG_m of two phases are equal

$$\Delta G_m(\text{isotropic}) = \Delta G_m(\text{nematic}) \tag{120}$$

The numerical analysis of the phase transition at constant force is shown in Fig. 14.

The chemical potentials of the solvent and the polymer at constant length or at constant force can also be calculated. The proper chemical potentials are partial derivatives of ΔA_m (or ΔG_m) with respect to the number of solvent n_1 and polymer n_2 molecules. The knowledge of the chemical potentials enables the study of the equilibrium phase coexistence conditions in stretched networks.

The numerical results show that the isotropic–nematic phase transition is possible only for the axial ratio x of the polymer segments within a certain range. If polymer segments have low axial ratio then the nematic phase never exists, irrespective of deformation. On the other hand, for sufficiently large value of x the system is always in the nematic phase, and the isotropic phase does not exist. For intermedium cases there is a possibility of isotropic–nematic phase transition at constant length or constant force. This is shown in Fig. 15 which shows that the isotropic–nematic phase transition is possible only within the certain range of values of x for which the plot of $\bar{y}/x$ vs. x has inverted 'S-like' shape. The phase transition is manifested by a sudden change of the orientation function S, and by the sharp minimum in the modulus as the function of the extension ratio α. The phase transition can also be driven by deswelling the system, and thus by changing the volume

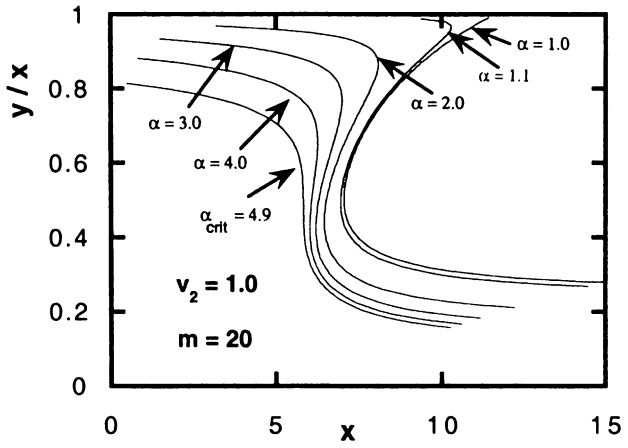

Fig. 15. The values of $\bar{y}/x$ as a function of x for several elongations α. For $x > 10.98$ the system is always anisotropic.

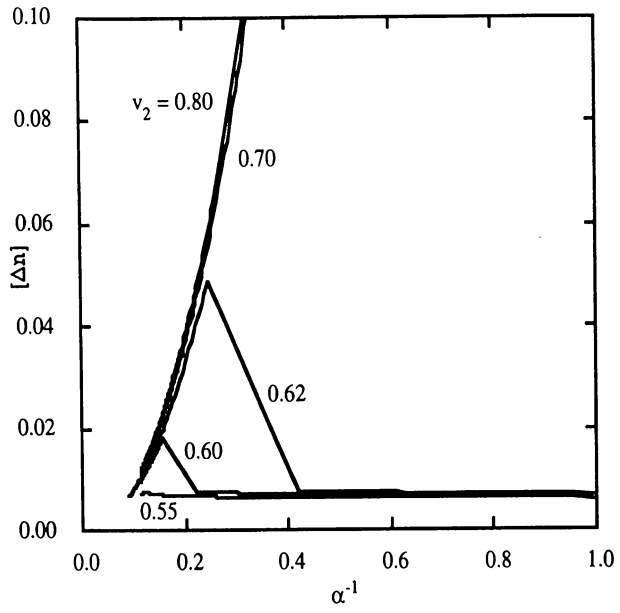

Fig. 16. The reduced birefringence as a function of the inverse elongation for a swollen network undergoing phase transition at constant stress. The calculations were performed for $x = 12$, $m = 100$ and for varying values of v_2.

fraction of the polymer at constant length (or constant force).

Yang et al. [80] applied this theory to study the optical properties of networks of semi-rigid chains. The optical birefringence in networks undergoing phase transitions at constant length, or constant force and photoelastic properties of networks of semirigid chains were calculated. The birefringence Δn of the network changes rapidly at the phase transition. It increases drastically with the extension during the phase transition. This is shown in Fig. 16. The discontinuity of the stress-optical coefficient C at the phase transition was also observed.

9. Strain-induced crystallization in elatometric networks

Some elastomeric networks undergo strain-induced crystallization; the system becomes spatially disordered and the formation of highly ordered crystallites is observed inside amorphous (disordered) network [81–84]. A thermodynamic theory for strain-induced crystallization was first developed by Flory [85]. Flory's theory is based on many simplifying assumptions. He assumed that the crystallites form parallel to the direction of stretch. He assumed also that the chains are Gaussian. The configurational probability of an amorphous Gaussian chain is

$$W(x,y,z) = (\beta/\pi^{1/2})^3 \exp[-\beta^2(x^2 + y^2 + z^2)] \tag{121}$$

with $\beta = (3/2n)^{1/2}/l$ where n is the number of statistical segments per chain, l is the length of a segment and x, y, and z are Cartesian components of the end-to-end vector $\mathbf{r}$. Under the affine deformation along the z-axis by a factor λ, the distribution of chain coordinates becomes

$$\Omega(x,y,z) = \nu(\beta/\pi^{1/2})^3 \exp\left[-\beta^2\left(\lambda x^2 + \lambda y^2 + \frac{z^2}{\lambda^2}\right)\right] \tag{122}$$

where ν is the total number of chains. Flory assumed that when η of the n segments of a chain crystallize, then the relative number of configurations available to the $n - \eta$ segments is

$$W'(x,y,z') = (\beta'/\pi^{1/2})^3 \exp[-\beta'^2(x^2 + y^2 + z'^2)] \tag{123}$$

with $\beta' = \beta[n/(n-\eta)]^{1/2}$ and $z' = \pm(|z| - \eta l)$, where z' is the algebraic sum of the displacement lengths of the two amorphous portions of the chain, with the plus sign for $z > 0$ and the minus for $z < 0$. The x and y displacements are unaffected. The distribution of the coordinates of ν chains becomes

$$\Omega'(x,y,z') = \nu W'(x,y,z') \tag{124}$$

The themodynamic analysis of Flory rests on the assumption that if $n - \eta$ segments of each of the chains melt, this leads to an entropy change

$$\Delta S_a = \nu(n - \eta)s_f \tag{125}$$

where s_f is the entropy of fusion per segment. He also assumed that because of the melting of the $n - \eta$ segments, there is an additional entropy change ΔS_b resulting from the change in the chain length distribution in the amorphous region

$$\Delta S_b = k\sum_{xyz} \Omega(xyz) \ln W'(x,y,z') - k\sum_{xyz} \Omega'(xyz') \ln W'(x,y,z') \tag{126}$$

Flory also assumed that the change in chain length distribution is not accompanied by a change in internal energy. Then the free energy A of the system with respect to a totally crystalline chain depends only on the entropic contributions. The configurational entropy of ν chains involved in crystallization is $\Delta S = \Delta S_a + \Delta S_b$ and the heat of fusion of $n - \eta$ segments of ν chains is $\nu h_f(n - \eta)$, i.e.

$$A = -\nu RT[h_f(n - \eta) + \Delta S_a + \Delta S_b \tag{127}$$

The thermodynamic condition for the equilibrium at the strain-induced crystallization is

$$\left(\frac{\partial A}{\partial \eta}\right)_{\lambda_x,\lambda_y,\lambda_z} = 0 \tag{128}$$

Flory calculated the effect of the strain on the elevation of the melting point, changes in the degree of crystallinity ω, and the elastic force exhibited by the network. The elevation

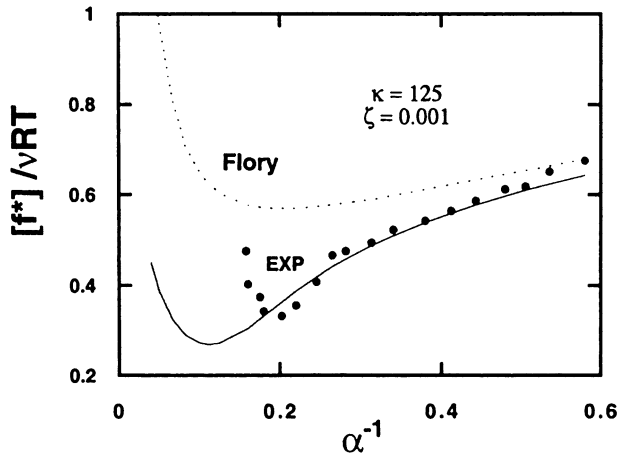

Fig. 17. Experimental values of the normalized reduced stresss $[f^*]/\nu kT$ vs. α^{-1} for *cis*-1-4 polybutadiene compared with predictions of the present theory ($\zeta = 0.001$ and $\kappa = 125$), and with those of Flory's theory.

of the melting point with strain predicted by the theory is

$$1/T_m = 1/T_m^0 - (R/H_f)\phi(\lambda) \tag{129}$$

The degree of crystallinity is

$$\omega = 1 - \{(3/2 - \phi(\lambda))/(3/2 - \theta)\}^{1/2} \tag{130}$$

and the retractive force f at equilibrium in a stretched polymer is given by

$$f = \nu RT[(\lambda - \lambda^{-2}) - (6n/\pi)^{1/2}\omega]/(1 - \omega) \tag{131}$$

where ν is the number of chains per unit volume.

Here

$$\phi(\lambda) = (6/\pi n)^{1/2}\lambda - (\lambda^2/2 + \lambda^{-1})/n \tag{132}$$

and

$$\theta = (H_f/R)(1/T_m^0 - 1/T) \tag{133}$$

where H_f is the molar heat of fusion per segment, and T_m^0 is the incipient crystallization temperature of the undeformed polymer.

In real networks end-to-end vectors of polymer chains do not deform affinely, as shown by Eq. (122). The distribution of instantaneous chain vectors is not affine in the strain. It is the convolution of the distribution of the mean vectors $\langle \mathbf{r} \rangle$ which is affine, and the distribution of fluctuations $\Delta \mathbf{r}$ which is independent of strain. A new theory of the strain-induced crystallization of polymers (based of the constrained junction theory of rubberlike elasticity) was developed to account for the effects of constraints [86,87]. The constrained junction theory assumes that the fluctuations are strain dependent and that the restrictions on the fluctuations are represented by a domain of constraints. The constraints depend on the network functionality ϕ, and also on the number of other chains sharing the same region of space. Real network shows behavior intermediate to the two extremes, namely the phantom and the affine models for the deformation. The Gaussian distribution function of the end-to-end distance in the presence of a domain of constraints becomes

$$\Omega(x,y,z) = \frac{\nu}{\Lambda_x\Lambda_y\Lambda_z}\left(\frac{\beta}{\pi^{1/2}}\right)^3 \times \exp\left[-\beta^2\left(\frac{x^2}{\Lambda_x^2} + \frac{y^2}{\Lambda_y^2} + \frac{z^2}{\Lambda_z^2}\right)\right] \tag{134}$$

where $\mathbf{\Lambda}$ is the macroscopic deformation tensor given by Eq. (98)

$$\Lambda_t^2 = \left(1 - \frac{2}{\varphi}\right)\lambda_t^2 + \frac{2}{\varphi}(1 + B_t) \quad (t = x,y,z)$$

with

$$B_t = (\lambda_t - 1)\left(\lambda_t + 1 - \zeta\lambda_t^2\right)/(1 + g_t)^2 \tag{135}$$

$$g_t = \lambda_t^2[\kappa^{-1} + \zeta(\lambda_t - 1)] \tag{136}$$

The parameter κ is a measure of the severity of the entanglement constraints and ζ takes into account the possibility of the transformation of the domains of constraints with increasing strain [34,88].

The calculation of the configurational entropy for network undergoing crystallization under stretching was carried out in the similar way as by Flory [85] starting from totally crystalline network. The calculations of the degree of crystallinity and the incipient crystallization temperature were also performed similarly as in the Flory's method.

The new theory shows much better agreement with experimental data on strain-induced crystallization than the original Flory theory, as shown by Fig. 17. Of course, the upswing in Fig. 17 could be also explained by other mechanisms, such as for example, the limited extensibility of real chains. Therefore the problem should be studied in more detail in the future, especially for other polymeric networks. Because *cis*-1,4 polybutadiene has always certain degree of crystallinity even when unstretched, natural rubber (which crystallizes significantly only when stretched) could be a better material for such studies.

10. Theoretical approach to filed polymer networks

Usually elastomers are compounded with a reinforcing filler. The most important examples are the addition of carbon black to natural rubber (in tires) and silica to silicone rubbers.

The addition of filler improves many properties of these materials like: the increase in modulus at given strain, tear and abrasion resistance, resilience, extensibility, tensile strength [89–93]. An experimental evidence suggest that the reinforcement effect depends on the size of filler particles with the maximum reinforcement obtained for particles

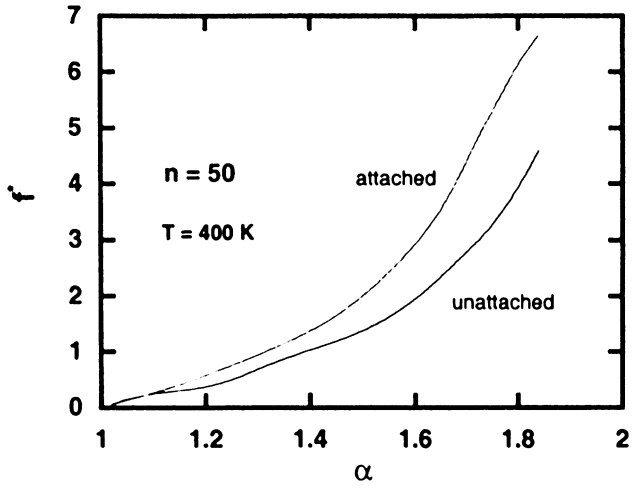

Fig. 18. Dependence of the nominal stress on the elongation for unattached PE chains composed of 50 bonds at temperature 400 K and the same chains attached to filler particles with specified diameters in Å.

size range of 10–100 nm. Large sized particles instead of reinforcement contribute to weakening of the polymer. The fillers have very complicated hierarchy of structures from aggregates through agglomerates to filler networking, with all of them showing highly irregular shapes. Polymer chains adsorb at the filler particle surface and covalent bonds are frequently formed. However, experimental data on carbon black and silica filled networks show that physical bonds play even much more important role than chemical bonding. Another factor which is closely related to the adsorption is the change of the distribution of end-to-end vectors of polymer chains in the presence of dispersed filler inside the elastomer. The excluded volume of the filler increases the non-Gaussian characteristics of nearby polymer chains.

The first theoretical attempt to explain the dependence of filled rubbers on the concentration of filler has been done by the Guth and Gold [94]. These authors modified the Einstein viscosity equation for spherical particles in a viscous medium by adding square term accounting for interactions between particles and obtained the equation

$$\eta = \eta_0(1 + 2.5\phi + 14.1\phi^2) \tag{137}$$

where η and η_0 are viscosities for filled and unfilled rubber and ϕ is volume fraction of filler. Eq. (137) has been generalized later by Guth to nonspherical particles [95]

$$\eta = \eta_0(1 + 0.67f\phi + 1.62f^2\phi^2) \tag{138}$$

where f is the shape factor used in the estimation of particles anisometry.

There are several other models of reinforcement in polymer composites [96]. Most of these theories are not molecular. There is a serious lack of rigorous extension of the statistical theory of rubber elasticity to a filled elastomer. A statistical model of filled network based on the replica formalism was developed by Heinrich and Vilgis [97].

The presence of the filler particles inside the polymer changes the distribution function of the end-to-end vector of the nearby chains, due to the excluded volume of the filler and due to the adsorption of chains on the filler surface. This leads to the change of elastic behavior of the polymer network. A molecular theory to study these effects was developed by Kloczkowski, Sharaf and Mark [98–101]. For simplicity the effect of adsorption was neglected in the theory. To calculate and compare the elastic properties of chains in unfilled networks and chains in the filled rubbers the Monte Carlo rotational isomeric state simulations for a single polymer chains were performed for polyethylene (PE) and poly(dimethyl)siloxane (PDMS) chains with various the degree of polymerization, and for different temperatures and different sizes of filler particles.

The method was based on the Monte Carlo calculations of the distribution of the end-to-end vector for free polymer chains, and for chains in the presence of the filler. The calculated end-to-end vector distribution functions enable the prediction of elastic properties of chains within the framework of Mark and Curro [102] theory.

The distribution $P(r)$ of the end-to-end vector obtained by Monte Carlo simulation is directly related to the Helmholtz free energy $A(r)$ of a chain with the end-to-end distance r

$$A(r) = c - kT \ln P(r) \tag{139}$$

where c is a constant.

The application of the three-chain model [102] leads to the following expression for the elastic free energy change during the deformation of the network, as the function of elongation ratio α

$$\Delta A = \frac{\nu}{3}[A(r_0\alpha) + 2A(r_0\alpha^{-1/2}) - 3A(r_0)] \tag{140}$$

Here ν is the number chains in the network and r_0 is the value of root-mean-square end-to-end vector of network chains. The simplifying assumption of affine deformation of the network chains was used in the derivation of Eq. (140). The normal stress f^* defined as the elastic force at equilibrium per unit cross-sectional area of the sample in the undeformed state is

$$f^* = -T\left(\frac{\partial \Delta A}{\partial \alpha}\right)_T \tag{141}$$

The substitution of Eq. (140) in to Eq. (141) gives

$$f^* = -\frac{\nu kTr_0}{3}[G'(r_0\alpha) - \alpha^{-3/2}G'(r_0\alpha^{-1/2})] \tag{142}$$

where $G(r) = \ln P(r)$, and $G'(r)$ denotes the derivative dG/dr.

The effect of the network reinforcement by filler is shown in Fig. 18 where the nominal stress as a function of elongation is plotted for PE chains for varying diameter of spherical filler particles. Because of the very simplified nature of the theory which neglects physical and chemical bonding between the polymer and the filler, the theory could

probably be the best applicable to non-aggregating fillers, such as, e.g. highly crosslinked microgels.

11. Discussions

The presented work covers most of the fields of equilibrium rubberlike elasticity. The research in this field has started in late thirties with the pioneering works by Kuhn, Guth and H.F. Mark. It became a very active field in forties and fifties with important contributions by Flory, James, Guth, Treloar, Wall and many other researchers, based mostly on the analysis of Gaussian chain models. The sixties and seventies were the times of the establishing the basis for the rigorous statistical mechanical treatment of polymers and elastomeric materials, with fundamental works by Flory and his collaborators, Volkenstein, Nagai and many other scientists. The rotational isomeric states model allowing the more realistic analysis of polymer chains was developed in that time period. In the seventies the computer simulations of polymers (including their elastic properties) became very important. With the advance in the computer technology the role of these simulations rapidly increased in the eighties and the nineties. The computer simulations of polymer chains were first based on the Monte Carlo method, but recently also the molecular dynamics of polymers became a standard simulation method.

In the eighties and nineties the rubberlike elasticity became a fully developed field of science. Many basic problems in this field has been has been already solved, and the further growth concentrates on technological aspects, such as finding better high performance materials, using elastomeric phases for the improvement of non-elastomeric materials (such as ceramics) or using the computer modeling for the development of new materials. The computer experiments are gradually replacing 'real' laboratory experiments in the polymer industry.

The unsolved problems and future directions in rubberlike elasticity include the studies of the effect of network topology, the strain-induced crystallization in unusual deformations, studies of molecular origins of reinforcement, refinement of the existing theories of constraints in networks and theories of segmental orientation, 'taylor-like' design of materials with desired properties.

The fields of rubberlike elasticity which are relatively undeveloped and have a large growth potential are biopolymers and bioelastomers. Fundamental problems for the future investigation include the study of the elastic properties of DNA chains, folding–unfolding transitions in single chains of muscle proteins (such as titin), the development of artificial muscles, controlled delivery of drugs and agricultural chemicals by gels, and many others. Recently it has been shown that ideas from the rubberlike elasticity theory can be successfully applied to the analysis of fluctuations of residues in compact proteins [103,104] and to the study of protein folding [105].

References

[1] Kuhn W. Kolloid Z 1936;76:258.
[2] Kuhn W. Angew Chem, Int Ed Engl 1938:51.
[3] Kuhn W. J Polym Sci 1946;1:380.
[4] Treloar LRG. Trans Faraday Soc 1946;42:77.
[5] Treloar LRG. The physics of rubber elasticity. 3rd ed. Oxford: Clarendon Press, 1975.
[6] Erman B, Mark JE. Structures and properties of rubberlike networks. Oxford: Oxford University Press, 1997.
[7] Cotton JP, Decker D, Benoit H, Farnoux B, Higgins J, Jannink G, Ober R, Picot C, des Cloizeaux J. Macromolecules 1974;7:863.
[8] Higgins JS, Benoit HC. Polymers and neutron scattering. Oxford: Clarendon Press, 1994.
[9] Erman B, Mark JE. Rubberlike elasticity. A molecular primer. New York: Wiley, 1988.
[10] James HM, Guth E. Ind Engng Chem 1941;33:624.
[11] James HM, Guth E. Ind Engng Chem 1942;34:1365.
[12] James HM, Guth E. J Chem Phys 1943;10:455.
[13] James HM, Guth E. J Appl Phys 1944;15:294.
[14] James HM. J Chem Phys 1947;15:651.
[15] James HM, Guth E. J Chem Phys 1947;15:669.
[16] James HM, Guth E. J Polym Sci 1949;4:153.
[17] James HM, Guth E. J Chem Phys 1953;21:1039.
[18] Flory PJ. Proc Roy Soc Lond 1976;A351:351.
[19] Eichinger BE. Macromolecules 1972;5:496.
[20] Pearson DS. Macromolecules 1977;10:696.
[21] Duiser J, Staverman AJ. Physics of non-crystalline solids. Amsterdam: North Holland, 1965.
[22] Staverman AJ. Adv Polym Sci 1982;44:73.
[23] Wall FT. J Chem Phys 1942;10:132.
[24] Wall FT. J Chem Phys 1942;10:485.
[25] Wall FT. J Chem Phys 1943;11:527.
[26] Flory PJ, Rehner J. J Chem Phys 1943;11:512.
[27] Flory PJ. Ind Engng Chem 1946;38:417.
[28] Flory PJ. J Chem Phys 1951;18:108.
[29] Wall FT, Flory PJ. J Chem Phys 1951;19:1435.
[30] Flory PJ. J Chem Phys 1977;66:5720.
[31] Ronaca G, Allegra G. J Chem Phys 1976;63:4990.
[32] Erman B, Flory PJ. Macromolecules 1982;15:806.
[33] Erman B, Flory PJ. J Chem Phys 1978;68:5363.
[34] Erman B, Flory PJ. Macromolecules 1982;15:800.
[35] Deam RT, Edwards SF. Phil Trans Roy Soc Lond 1976;280:317.
[36] Ball RC, Doi M, Edwards SF. Polymer 1981;22:1010.
[37] Kloczkowski A, Mark JE, Erman B. Macromolecules 1989;22:1423.
[38] Kloczkowski A. In: Mark JE, editor. Physical properties of polymer networks. Woodbury, NY: American Institute of Physics, 1996.
[39] Edwards SF, Vilgis T. Rep Prog Phys 1988;51:243.
[40] Picot C. Prog Colloid Pol Sci 1987;75:83.
[41] Ullman R. J Chem Phys 1979;71:436.
[42] Ullman R. Macromolecules 1982;15:1395.
[43] Kloczkowski A, Mark JE, Erman B. Macromolecules 1989;22:4502.
[44] Kloczkowski A, Mark JE, Erman B. Macromolecules 1992;25:2455.
[45] Kloczkowski A, Mark JE, Erman B. Comput Polym Sci 1992;2:8.
[46] Bastide J, Herz J, Boue F. J Phys (Paris) 1985;46:1967.
[47] Bastide J. Physics of finely divided matter, Springer Proceedings in Physics, vol. 5. New York: Springer, 1985.
[48] Bastide J, Boue F. Physica 1986;140A:251.
[49] Sharaf MA, Mark JE. Macromol Rep 1991;1:67.
[50] Higgs PG, Ball RC. J Phys (Paris) 1988;49:1785.
[51] Kloczkowski A, Mark JE, Erman B. Macromolecules 1991;23:3266.
[52] Rouse PE. J Chem Phys 1953;21:1272.
[53] Doi M, Edwards SF. The theory of polymer dynamics. Oxford: Oxford University Press, 1986.
[54] Zimm BH. J Chem Phys 1956;24:269.
[55] Chompff AJ, Prins W. J Chem Phys 1968;48:235.
[56] Chompff AJ. J Chem Phys 1970;53:1566, also p. 1577.

[57] Graessley WW. Macromolecules 1980;13:372.
[58] Kloczkowski A, Mark JE, Frisch HL. Macromolecules 1990;23:3481.
[59] Heinrich G, Dumler HB. Rubber Chem Technol 1998;71:53.
[60] Heinrich G. Rubber Chem Technol 1997;70:1.
[61] Erman B, Monnerie L. Macromolecules 1988;22:3342.
[62] Erman B, Monnerie L. Macromolecules 1992;25:4456.
[63] Kloczkowski A, Mark JE, Erman B. Macromolecules 1995;28:5089.
[64] Kloczkowski A, Mark JE, Erman B. Comput Polym Sci 1995;5:37.
[65] Volkenstein MW. Configurational statistics of polymeric chains. New York: Interscience, 1963.
[66] Nagai K. J Chem Phys 1964;40:2818.
[67] Flory PJ. Statistical mechanics of chain molecule. New York: Interscience, 1969.
[68] Riande E, Saiz E. Dipole moments and birefringence of polymers. Englewood Cliffs, NJ: Prentice Hall, 1992.
[69] Gent AN. Macromolecules 1969;2:262.
[70] Khun W, Grun F. Kolloid Z 1941;101:248.
[71] DiMarzio EA. J Chem Phys 1962;36:1563.
[72] Tanaka T, Allen G. Macromolecules 1977;10:426.
[73] Jarry JP, Monnerie L. Macromolecules 1979;12:316.
[74] Flory PJ. Macromolecules 1978;11:1141.
[75] Erman B, Bahar I, Kloczkowski A, Mark JE. Macromolecules 1990;23:5335.
[76] Flory PJ, Ronca G. Mol Cryst Liq Cryst 1979;54:289.
[77] Flory PJ, Ronca G. Mol Cryst Liq Cryst 1979;54:311.
[78] Kloczkowski A, Mark JE, Erman B. Macromolecules 1990;23:5035.
[79] Kloczkowski A, Mark JE, Erman B, Bahar I. Polymer blends, solutions and interfaces. In: Noda I, Rubingh DN, editors. Studies in polymer science, vol. 11. Amsterdam: Elsevier, 1992. p. 221.
[80] Yang Y, Kloczkowski A, Mark JE, Erman B, Bahar I. Macromolecules 1995;28:4920.
[81] Gent AN. J Polym Sci 1965;3A:3787.
[82] Gent AN. J Polym Sci 1966;4A:447.
[83] Mark JE. In: Mark JE, Eisenberg A, Graesley WW, Mandelkern L, Samulski ET, Koenig JL, Wignall GD, editors. Physical properties of polymers, 2nd ed. Washington, DC: American Chemical Society, 1993.
[84] Mandelkern L. Crystallization of polymers. New York: McGraw-Hill, 1964.
[85] Flory PJ. J Chem Phys 1947;15:397.
[86] Sharaf MA, Kloczkowski A, Mark JE. Comput Polym Sci 1992;2:84.
[87] Kloczkowski A, Mark JE, Sharaf MA, Erman B. In: Aharoni SM, editor. Synthesis, Characterization and theory of polymeric networks and gels. New York: Plenum Press, 1992. p. 227.
[88] Erman B, Flory P. Macromolecules 1983;16:1601.
[89] Kraus G. Adv Polym Sci 1971;8:155.
[90] Rigbi Z. Adv Polym Sci 1980;36:21.
[91] Donnet JB, Vidal A. Adv Polym Sci 1986;76:103.
[92] Kraus G, editor. Reinforcement of elastomers. New York: Interscience, 1965.
[93] Mark JE. Kautsch, Gummi, Kunst 1989;42:191.
[94] Guth E, Gold O. Phys Rev 1938;53:322.
[95] Guth E. J Appl Phys 1945;16:20.
[96] Ahemd S, Jones FR. J Mater Sci 1990;25:4933.
[97] Heinrich G, Vilgis TA. Macromolecules 1993;26:1109.
[98] Kloczkowski A, Sharaf MA, Mark JE. Comput Polym Sci 1993;3:39.
[99] Kloczkowski A, Sharaf MA, Mark JE. Chem Engng Sci 1994;17:2889.
[100] Wang Q, Kloczkowski A, Mark JE, Sharaf MA. J Polym Sci: Polym Phys Ed 1996;34:1647.
[101] Sharaf MA, Kloczkowski A, Mark JE. Comput Theor Polym Sci 2001 in press.
[102] Mark JE, Curro JG. J Chem Phys 1983;79:5705.
[103] Haliloglu T, Bahar I, Erman B. Phys Rev Lett 1997;79:3090.
[104] Bahar I, Aligtan AR, Erman B. Fold Des 1997;2:173.
[105] Erman B, Dill KA. J Chem Phys 2000;112:1050.
[106] Brodowsky H, Prager S. J Chem Phys 1963;39:1103.
[107] Paul B, Schulz M, Frisch HL. Comput Theor Polym Sci 1999;9:193.
[108] Gurtovenko AA, Gotlib YY. Macromolecules 1998;31:5756.
[109] Gotlib YY. Macromol Symp 1999;146:81.
[110] Gurovenko AA, Gotlib YY. Macromolecules 2000;33:6578.
[111] Gotlib YY, Gurovenko AA, Kilian HG. Polym Sci Ser A 2001;43:308.
[112] Gurovenko AA, Gotlib YY, Kilian HG. Macromol Theor Simul 2000;9:388.
[113] Meyer KH, von Susich G, Valko E. Kolloid Z 1932;59:208.
[114] Guth E, Mark H. Monasch 1934;65:93.
[115] Flory PJ. Br Polym J 1985;17:96.
[116] Kaestner S. Faserforschung Textiltechnik/Z Polymerforschung 1976;27:1.
[117] Kaestner S. Colloid Polym Sci 1981;259:499.
[118] Kaestner S. Colloid Polym Sci 1981;259:508.
[119] Burchard W. Ber Bunsenges Phys Chem 1985;89:1154.
[120] Heinrich G, Straube E, Helmis G. Adv Polym Sci 1985;85:1154.
[121] Warner M, Edwards SF. J Phys A 1978;11:1649.
[122] Urayama K, Kawamura T, Hirata Y, Kohjiya S. Polymer 1998;39:3827.
[123] Beck Tan NC, Bauer BJ, Plestil J, Barnes JD, Liu D, Matejka L, Dusek K, Wu WL. Polymer 1999;40:4603.
[124] Kremer K, Grest GS. In: Binder K, editor. Monte Carlo and molecular dynamics simulations in polymer science. New York: Oxford University Press, 1995. p. 194.
[125] Duerling ER, Kremer K, Grest GS. Phys Rev Lett 1991;67:3531.
[126] Sommer JU, Schulz M, Trautenberg HL. J Chem Phys 1993;98:7515.
[127] Grest GS, Puetz M, Everaers R, Krerner K. J Non-Cryst Solids 2000;274:139.
[128] Everaers R, Kremer K. Macromol Symp 1995;93:53.
[129] Everaers R. New J Phys 1999;1:12.1.
[130] Everaers R, Kremer K. Macromolecules 1995;28:7291.
[131] Duerling ER, Kremer K, Grest GS. J Chem Phys 1994;101:8169.
[132] Everaers R, Kremer K. Phys Rev E 1996;53:R37.
[133] Muthukumar M, Nickel BG. J Chem Phys 1984;80:5839.
[134] Muthukumar M, Nickel BG. J Chem Phys 1987;86:460.
[135] Freed KF. Renormalization group theory of macromolecules. New York: Wiley, 1987.
[136] Edwards SF. Proc Phys Soc 1967;92:9.
[137] de Gennes PG. J Chem Phys 1971;55:572.
[138] de Gennes PG. Scaling concepts in polymer physics. Ithaca, NY: Cornell University Press, 1979.
[139] Marrucci G. Macromolecules 1981;14:434.
[140] Gaylord RJ, Douglas JF. Polym Bull 1987;18:347.
[141] Gaylord RJ, Douglas JF. Polym Bull 1990;23:529.
[142] Rubinstein M, Panyukov S. Macromolecules 1997;30:8036.
[143] Eichinger BE. Macromolecules 1977;10:671.
[144] Eichinger BE, Martin JE. J Chem Phys 1978;69:4595.
[145] Eichinger BE. Macromolecules 1980;13:1.
[146] Dossin LM, Graessley WW. Macromolecules 1979;12:123.
[147] Pearson DS, Graessley WW. Macromolecules 1980;13:1001.
[148] Langley NR. Macromolecules 1968;1:348.
[149] Graessley WW. Adv Polym Sci 1982;47:67.
[150] Edwards SF, Vilgis TA. Polymer 1986;27:483.
[151] Marzocca AJ, Matteo CL, Gonazales JJ, Raymondo RB. J Phys IV Coll 1996;C8:583.
[152] Westerman S, Phyckhout-Hintzen W, Richter D. Macromolecules 2001;34:2186.
[153] Westerman S, Kreitschmann M, Pyckhout-Hintzen W, Richter D, Straube E, Farago B, Goerigk G. Macromolecules 1999;32:5793.
[154] Urayama K, Kawamura T, Kohjiya S. Preprint.
[155] Gottelib M, Gaylord R. Macromolecules 1987;20:130.